Article:

Aad, G. orcid.org/0000-0002-6665-4934, Aakvaag, E. orcid.org/0000-0001-7616-1554, Abbott, B. orcid.org/0000-0002-5888-2734 et al. (2930 more authors) (2025) Diferential cross-section measurements of D± and D±s meson production in proton-proton collisions at √s = 13 TeV with the ATLAS detector. Journal of High Energy Physics, 2025. 86. ISSN 1126-6708

https://doi.org/10.1007/jhep07(2025)086

Published for SISSA by Springer

Received: *January 7, 2025*
Accepted: *May 23, 2025*
Published: *July 4, 2025*

Differential cross-section measurements of $D^{\pm}$ and $D_s^{\pm}$ meson production in proton-proton collisions at $\sqrt{s} = 13$ TeV with the ATLAS detector

The ATLAS collaboration

E-mail: atlas.publications@cern.ch

Abstract: The production of $D^{\pm}$ and $D_s^{\pm}$ charmed mesons is measured using the $D^{\pm}/D_s^{\pm} \to \phi(\mu\mu)\pi^{\pm}$ decay channel with 137 fb^{-1} of $\sqrt{s} = 13$ TeV proton-proton collision data collected with the ATLAS detector at the Large Hadron Collider during the years 2016–2018. The charmed mesons are reconstructed in the range of transverse momentum $12 < p_T < 100$ GeV and pseudorapidity $|\eta| < 2.5$. The differential cross-sections are measured as a function of transverse momentum and pseudorapidity, respectively, and compared with next-to-leading-order QCD predictions. The predictions are found to be consistent with the measurements in the visible kinematic region within the large theoretical uncertainties.

Keywords: B Physics, Hadron-Hadron Scattering

ArXiv ePrint: 2412.15742

https://doi.org/10.1007/JHEP07(2025)086

JHEP07(2025)086

Contents

1 Introduction

The production of heavy hadrons in proton-proton collisions is a fundamental process that provides a crucial test of perturbative quantum chromodynamics (QCD) calculations. However, large uncertainties persist in current theoretical predictions due to the fact that the masses of heavy quarks are comparable to the typical energy scales of the hard scattering processes [1, 2]. Moreover, heavy hadrons can be produced promptly via the hadronisation of charm quarks from the initial hard scattering process, or non-promptly in decays of b-hadrons; precise predictions of such processes are challenging, due to difficulties in modelling non-perturbative effects such as hadronisation, as well as uncertainties in the fragmentation functions and decay dynamics of heavy-flavour hadrons. Given the sizeable theoretical uncertainties, experimental constraints on heavy hadron production cross-sections are important to improve calculation techniques, as well as in searches for new physics phenomena, where heavy hadron production is often either a signal process or a significant background process. For instance, several charmed and bottom mesons have significant decay branching ratios to τ-lepton final states [3]; precise cross-section measurements are necessary for using such decays to search for lepton-flavour-violating τ-lepton decays [4] at the Large Hadron Collider (LHC) [5].

At the LHC, prompt and non-prompt D meson[1] production in proton-proton (pp) collisions has been measured by different experiments. The ALICE Collaboration reported

[1]In this paper, the $\pm$ symbol is used to represent both charge conjugates inclusively for different D mesons; the D^0 symbol is used to represent D^0 and $\bar{D}^0$ mesons inclusively.

the differential production cross-sections of prompt D^0, $D^{\pm}$, $D^{*\pm}$, and $D_s^{\pm}$ mesons at a centre-of-mass energy of $\sqrt{s} = 13$ TeV, in the mid-rapidity region and in different ranges of transverse momentum, p_T; in particular, the $D^{\pm}$ meson cross-section was measured up to p_T of 50 GeV and the $D_s^{\pm}$ meson cross-section was measured up to p_T of 36 GeV [6]. Recently, the ALICE Collaboration published differential production cross-sections of non-prompt D^0, $D^{\pm}$ and $D_s^{\pm}$ mesons in the range of $p_T < 24$ GeV; the results are compared to the prompt measurements to evaluate the non-prompt production fraction [7]. Previously, the ALICE Collaboration also published measurements of D meson production at $\sqrt{s} = 2.76$, 5.02, and 7 TeV [8–11]. A study conducted by the CMS Collaboration reported the differential cross-sections of $D^{*\pm}$, D^0, and $D^{\pm}$ with p_T up to 100 GeV based on a partial data sample at $\sqrt{s} = 13$ TeV collected in 2016 [12]. The LHCb Collaboration published measurements of the production cross-sections of prompt D^0, $D^{\pm}$, $D^{*\pm}$, and $D_s^{\pm}$ mesons in the range of $p_T < 15$ GeV in the forward region using $\sqrt{s} =$ 13 TeV data [13]. Similarly, the LHCb Collaboration published measurements of D meson production at $\sqrt{s} = 5$ and 7 TeV [14, 15]. The ATLAS Collaboration has measured $D^{*\pm}$, $D^{\pm}$, and $D_s^{\pm}$ meson production at $\sqrt{s} = 7$ TeV [16], but no such measurement has been performed at $\sqrt{s} = 13$ TeV, and the differential cross-section of the $D_s^{\pm}$ meson has not been measured.

This paper presents a measurement of $D^{\pm}$ and $D_s^{\pm}$ meson differential production cross-sections performed with the ATLAS detector using the pp collision data at $\sqrt{s} = 13$ TeV collected during the years 2016–2018. To measure the $D^{\pm}$ and $D_s^{\pm}$ mesons produced at the LHC, this study makes use of decay channels $D^{\pm}/D_s^{\pm} \to \phi(\mu\mu)\pi^{\pm}$ with semileptonic final states. In comparison to reconstructing the fully hadronic decays of the D mesons, the selected decay channels make use of the precise muon reconstruction and identification in the ATLAS detector, allowing a much cleaner signature with a lower background level. The final state of two muons and one pion ($\mu\mu\pi$) is fully reconstructed and identified, to construct the D meson decay vertex. The yields of the $D^{\pm}$ and $D_s^{\pm}$ meson signals are then extracted simultaneously by fitting the invariant mass distributions of the $\mu\mu\pi$ system.

To calculate the production cross-sections, simulated events are used to evaluate the reconstruction efficiencies and acceptance. Because of the difficulties in separating the D mesons produced by an initial charm quark (prompt) and those produced by an initial bottom quark (non-prompt), this study does not attempt to extract the prompt and non-prompt signal yields separately; however, their relative contributions in simulated events are constrained to match the data by fitting the pseudo-proper lifetime distribution. The yields and the cross-sections presented are inclusive of both prompt and non-prompt D mesons, unless otherwise specified.

The inclusive and differential cross-sections of the $D^{\pm}$ and $D_s^{\pm}$ mesons are reported in the range of $|\eta| < 2.5$ and $12 < p_T < 100$ GeV and compared with state-of-the-art next-to-leading-order (NLO) calculations. This is the first differential measurement of the $D_s^{\pm}$ meson production reported by the ATLAS Collaboration, and the first time such a measurement has been performed up to transverse momenta of 100 GeV at the LHC.

2 ATLAS detector

The ATLAS detector [17] at the LHC covers nearly the entire solid angle around the collision point.[2] It consists of an inner tracking detector surrounded by a thin superconducting solenoid, electromagnetic and hadronic calorimeters, and a muon spectrometer incorporating three large superconducting air-core toroidal magnets.

The inner-detector system (ID) is immersed in a 2 T axial magnetic field and provides charged-particle tracking in the range $|\eta| < 2.5$. The high-granularity silicon pixel detector covers the vertex region and typically provides four measurements per track, the first hit generally being in the insertable B-layer (IBL) installed before Run 2 [18, 19]. It is followed by the SemiConductor Tracker (SCT), which usually provides eight measurements per track. These silicon detectors are complemented by the transition radiation tracker (TRT), which enables radially extended track reconstruction up to $|\eta| = 2.0$. The TRT also provides electron identification information based on the fraction of hits (typically 30 in total) above a higher energy-deposit threshold corresponding to transition radiation.

The calorimeter system covers the pseudorapidity range $|\eta| < 4.9$. Within the region $|\eta| < 3.2$, electromagnetic calorimetry is provided by barrel and endcap high-granularity lead/liquid-argon (LAr) calorimeters, with an additional thin LAr presampler covering $|\eta| < 1.8$ to correct for energy loss in material upstream of the calorimeters. Hadronic calorimetry is provided by the steel/scintillator-tile calorimeter, segmented into three barrel structures within $|\eta| < 1.7$, and two copper/LAr hadronic endcap calorimeters. The solid angle coverage is completed with forward copper/LAr and tungsten/LAr calorimeter modules optimised for electromagnetic and hadronic energy measurements respectively.

The muon spectrometer (MS) comprises separate trigger and high-precision tracking chambers measuring the deflection of muons in a magnetic field generated by the superconducting air-core toroidal magnets. The field integral of the toroids ranges between 2.0 and 6.0 T m across most of the detector. Three layers of precision chambers, each consisting of layers of monitored drift tubes, cover the region $|\eta| < 2.7$, complemented by cathode-strip chambers in the forward region, where the background is highest. The muon trigger system covers the range $|\eta| < 2.4$ with resistive-plate chambers in the barrel, and thin-gap chambers in the endcap regions.

The luminosity is measured mainly by the LUCID–2 [20] detector that records Cherenkov light produced in the quartz windows of photomultipliers located close to the beampipe.

Events are selected by the first-level trigger system implemented in custom hardware, followed by selections made by algorithms implemented in software in the high-level trigger [21]. The first-level trigger accepts events from the 40 MHz bunch crossings at a rate below 100 kHz, which the high-level trigger further reduces in order to record complete events to disk at about 1 kHz.

[2] ATLAS uses a right-handed coordinate system with its origin at the nominal interaction point (IP) in the centre of the detector and the z-axis along the beam pipe. The x-axis points from the IP to the centre of the LHC ring, and the y-axis points upwards. Polar coordinates (r, ϕ) are used in the transverse plane, ϕ being the azimuthal angle around the z-axis. The pseudorapidity is defined in terms of the polar angle θ as $\eta = -\ln\tan(\theta/2)$ and is equal to the rapidity $y = \frac{1}{2}\ln\left(\frac{E+p_z}{E-p_z}\right)$ in the relativistic limit. Angular distance is measured in units of $\Delta R \equiv \sqrt{(\Delta y)^2 + (\Delta\phi)^2}$.

JHEP07(2025)086

A software suite [22] is used in data simulation, in the reconstruction and analysis of real and simulated data, in detector operations, and in the trigger and data acquisition systems of the experiment.

3 Data sample, event simulation and theoretical predictions

The data used in this analysis were collected in 2016–2018 with the ATLAS detector in pp collisions at $\sqrt{s} = 13\,\text{TeV}$ at the LHC. Data collected during 2015 were not used for this study, because of the unavailability of low-p_{T} di-muon triggers in the di-muon invariant mass range of interest. The data are selected after requiring each detector component to be fully operational [23]. The analysed data sample corresponds to an integrated luminosity of $137\,\text{fb}^{-1}$ [24].

To model inelastic events produced in pp collisions, a large sample of Monte Carlo (MC) simulated events was prepared using the Pythia 8.212 [25] event generator. The simulation was performed using leading-order (LO) matrix elements for all $2 \to 2$ QCD processes. Initial-state and final-state parton showering were used to simulate the effect of higher-order processes. The NNPDF2.3lo [26] parameterisation provided the parton distribution functions (PDF) of the proton. The charm quark and bottom quark masses were set to 1.5 GeV and 4.8 GeV, respectively. The event sample was simulated using the ATLAS A14 set of tuned parameters [27]. Separate samples were generated for $pp \to c\bar{c}$ and $pp \to b\bar{b}$ processes, corresponding to prompt and non-prompt production of D mesons, respectively. The generated $D^{\pm}$ and $D_s^{\pm}$ mesons were decayed into $\phi(\mu\mu)\pi^{\pm}$. The generated events were passed through a full ATLAS detector simulation [28] based on Geant4 [29] and processed with the same reconstruction algorithms as used for the data. The generation of the simulated event samples includes the effect of multiple pp interactions per bunch crossing (pile-up), as well as the effect on the detector response due to interactions from bunch crossings before or after the one containing the hard interaction. The effect of pile-up was modelled by overlaying the simulated hard-scattering event with inelastic pp collisions generated with Pythia 8.186 [30] using the NNPDF2.3lo PDF set and the A3 set of tuned parameters [31]. The simulated events were processed through the same reconstruction algorithms as used for the data.

The measured cross-sections are compared with the general-mass variable-flavour-number scheme (GM-VFNS) [1, 32–35] and the fixed-order next-to-leading-logarithm (FONLL) [36, 37] predictions. These calculations provide more reliable predictions than the traditional NLO massive and massless calculations in the intermediate and high transverse momentum range, where the heavy quark mass, m_Q, is not negligible compared to the transverse momentum of the quark, $p_{\mathrm{T}Q}$. Most of the setup for GM-VFNS and FONLL is unchanged as described in the previous ATLAS measurements [16]; the only updates are the PDF set and the fragmentation fractions used in the FONLL predictions.

The GM-VFNS prediction aims to combine the massless scheme with the massive scheme. In the calculation, the charm quark PDF evolves with massless evolution, while the heavy quark mass is retained in the hard-scattering calculation. With such an approach, the calculation agrees with the massless scheme at $p_{\mathrm{T}Q} \gg m_Q$, and with the massive scheme at $p_{\mathrm{T}Q} \approx m_Q$. The GM-VFNS calculation uses the CT14nlo [38] PDF set and the fragmentation functions are taken from the KKKS08 set [39]. The prediction is available for both $D^{\pm}$ and $D_s^{\pm}$ mesons; the inclusive (prompt and non-prompt) values are provided by the authors themselves. The uncertainties in the GM-VFNS predictions are dominated by QCD scale uncertainties, namely those of the renormalisation and factorisation scales for initial-state singularities and of the factorisation scale for final-state singularities.

The FONLL calculation consists of three components: the heavy quark production cross-section calculated in perturbative QCD, the non-perturbative heavy-flavour fragmentation, and the decay function describing the heavy hadron decay into leptons. The principle of FONLL is to expand the massless scheme computation in powers of the strong coupling $\alpha_{\rm s}$, and replace a finite number of terms with their massive scheme counterparts. For instance, the massive and massless scheme predictions are matched exactly up to $O(\alpha_{\rm s}^3)$, giving predictions that are reliable for both $p_{{\rm T}Q} \approx m_Q$ and $p_{{\rm T}Q} \gg m_Q$ regions. Currently, the FONLL calculation is available for the $D^{\pm}$ meson, but not for the $D_s^{\pm}$ meson [36, 37, 40, 41]. The calculation uses the NNPDF3.0NLO [42] PDF set, and the fragmentation fractions $f(b/c \to D)$ are taken from averaging the LEP measurements [43]. The fragmentation fractions, updated by the author of ref. [43] using the newest values of charmed hadron decay branching ratios in ref. [3], are $f(b \to D^{\pm}) = 0.217 \pm 0.011$ and $f(c \to D^{\pm}) = 0.219 \pm 0.010$.[3] The theoretical uncertainties considered include the renormalisation and factorisation scale uncertainties, the pole-mass uncertainties of charm and bottom quarks, the PDF uncertainty, and the fragmentation-fraction uncertainty.

For both GM-VFNS and FONLL, the inclusive cross-sections at $\sqrt{s} = 13\,\text{TeV}$ are also compared with the corresponding values at $\sqrt{s} = 7\,\text{TeV}$ in the same fiducial volume. In such comparisons, the scale uncertainties at different centre-of-mass energies are assumed to be fully correlated, in order to evaluate the ratios between cross-sections at different centre-of-mass energies.

4 Event reconstruction and selection

To identify and select the decay $D^{\pm}/D_s^{\pm} \to \phi(\mu\mu)\pi^{\pm}$, a series of selection criteria are defined to enhance the signal-to-background ratio; the selections are summarised in table 1. The events are first required to have been accepted by two-muon triggers, which pre-selected muons with certain $p_{\rm T}$ thresholds and a loose di-muon invariant mass requirement. At least one of the two muons was required to satisfy a $p_{\rm T}$ threshold of 6 GeV; the threshold for the other muon was either 6 GeV or 11 GeV, depending on the year of data-taking [44]. Combined ID+MS measurements of track parameters are used to reconstruct muons; they are required to have $p_{\rm T}$ greater than 6 GeV, to be within the pseudorapidity range of $|\eta| < 2.5$, and to satisfy the *Loose* identification working point requirements [45]. Di-muon candidates are also required to contain two selected muons with opposite electric charges Q_{μ}. The di-muon invariant mass is required to agree with the ϕ meson mass of 1 019.5 MeV [3] within a window

[3] In this paper, the fragmentation fractions obtained by averaging the LEP measurements are used, because the $p_{\rm T}$ range of interest is relatively high compared to the $D^{\pm}$ and $D_s^{\pm}$ meson masses. It is also noted that the ALICE Collaboration has measured the fragmentation fractions in the low-$p_{\rm T}$ range, where the $p_{\rm T}$ of the quarks is comparable to the mass of the hadrons ($p_{{\rm T}Q} \approx m_Q$). If the fragmentation values obtained by the ALICE Collaboration were used, the FONLL prediction would be lowered by approximately 10%.

Selection	
Muon objects	Two muons satisfying the *Loose* [45] working point
Track object	One track satisfying the *Loose* [46] working point
Transverse momentum	$p_{\mathrm{T}}^{\mu} > 6\,\mathrm{GeV}$, $p_{\mathrm{T}}^{\pi} > 1\,\mathrm{GeV}$
Opposite charge muons	$Q_{\mu_1} \times Q_{\mu_2} = -1$
Total charge	$\lvert Q_{\mu\mu\pi} \rvert = 1$
Di-muon invariant mass	$\lvert m_{\mu\mu} - m_{\phi} \rvert < \delta m(\lvert\eta\rvert)$
L_{xy} significance	$\mathrm{Sig}(L_{xy}) > 3$
a_{xy}^0 significance	$\lvert \mathrm{Sig}(a_{xy}^0) \rvert < 4$
Vertex p-value	$\log(p_0^{\mathrm{vertex}}) > -0.8$
Highest vertex p-value	The vertex with $\mathrm{Max}(p_0^{\mathrm{vertex}})$ in the event

Table 1. Summary of selection requirements, with items defined in the text.

$\delta m(|\eta|)$ that scales linearly as a function of absolute pseudorapidity $|\eta|$, from 24 MeV at $|\eta| = 0$ to 48 MeV at $|\eta| = 2.5$. This requirement retains approximately 90% of di-muon signal events in MC simulated events. In addition, one track satisfying the *Loose* identification working point requirements [46], with p_{T} of at least 1 GeV and within the pseudorapidity range of $|\eta| < 2.5$, is required to be reconstructed in the ID.

All possible di-muon-plus-track ($\mu\mu\pi$) combinations that satisfy the total charge requirement $|Q_{\mu\mu\pi}| = 1$ are used as inputs to D meson candidate secondary vertex (SV) fits, to maximize the number of vertex candidates. For each candidate, a primary vertex (PV) refit [47] is performed after removing the three tracks associated to the candidate, providing an updated PV position. Due to the $D^{\pm}$ and $D_s^{\pm}$ lifetime, the three-particle SV is often separated from the primary vertex. The characteristics of the separation between the SV and the PV are therefore used to reject background. Two projections of the SV displacement relative to the PV in the transverse plane are used: $L_{xy} = |\vec{L}_{\mathrm{T}}| \cos\theta_{\mathrm{xy}}$ and $a_{xy}^0 = |\vec{L}_{\mathrm{T}}| \sin\theta_{xy}$, where $\vec{L}_{\mathrm{T}}$ is the vector connecting the PV and the SV in the transverse plane, and θ_{xy} is the angle between $\vec{L}_{\mathrm{T}}$ and the transverse momentum $\vec{p_{\mathrm{T}}}$ of the $\mu\mu\pi$ candidate. Since a large separation in L_{xy} distributions is observed between signal and background events, a stringent cut is placed on this variable. For a_{xy}^0, the background distribution has a tail similar to the non-prompt signal. To account for detector resolution, the significance of L_{xy} and a_{xy}^0, $\mathrm{Sig}(L_{xy})$ and $\mathrm{Sig}(a_{xy}^0)$, are defined as $L_{xy}/\sigma_{L_{xy}}$ and $a_{xy}^0/\sigma_{a_{xy}^0}$, where $\sigma_{L_{xy}}$ and $\sigma_{a_{xy}^0}$ are the uncertainties in L_{xy} and a_{xy}^0, respectively. The selections placed on these two variables are $\mathrm{Sig}(L_{xy}) > 3$ and $|\mathrm{Sig}(a_{xy}^0)| < 4$.

Given the large number of low-p_{T} tracks originating from hadronic activity, many tracks that are not produced by D meson decays are mistakenly included as candidates. To suppress these combinatorial backgrounds, which are often poorly reconstructed, requirements are placed on the goodness of fits for the SV. The SV p-value p_0^{vertex} is defined as the probability of obtaining a χ^2 value larger than that of the reconstructed SV; only SVs with $\log(p_0^{\mathrm{vertex}}) > -0.8$ (i.e. $p_0^{\mathrm{vertex}} > 0.158$) are selected. Because of the detector coverage and the trigger thresholds,

JHEP07(2025)086

the final candidate is required to have p_{T} above 12 GeV and to be within the pseudorapidity range of $|\eta| < 2.5$. In the following sections, p_{T} and η will refer to the transverse momentum and pseudorapidity of the $\mu\mu\pi$ system unless otherwise specified. At the end of the selection chain, only the $\mu\mu\pi$ candidate with the highest vertex fit probability p-value p_0^{vertex} is selected per event.

5 Signal extraction and cross-section measurement

To extract the signal, the invariant mass of the di-muon-plus-track candidates $m_{\mu\mu\pi}$ is constructed. The yields of the D mesons are then extracted by performing fits to the distributions of $m_{\mu\mu\pi}$ in bins of p_{T} and $|\eta|$; the model for this fit is described in section 5.1. Since evaluating the differential cross-section requires reconstruction efficiencies in multiple bins, such values are derived from MC simulated events. The reconstruction efficiencies are different for D mesons produced promptly and non-promptly, of which the relative contributions can be poorly modelled in MC simulation; therefore, an additional study is performed to constrain the fraction of non-prompt production from data. This involves extracting the signal yields in bins of pseudo-proper lifetimes and fitting the resulting distributions with templates from MC simulated events corresponding to prompt and non-prompt production; this procedure is described in section 5.2. Finally, the cross-section calculation is described in section 5.3.

5.1 Invariant mass fit model

Since a fit to the invariant mass $m_{\mu\mu\pi}$ is used to extract the signal yield in bins of p_{T}, η, and lifetime, the fit model must be flexible and stable enough to extract yields in subsets of data with different sample sizes and signal-to-background ratios. For the $D^{\pm}$ and $D_s^{\pm}$ signals, the fit models $P_{D^{\pm}}$ and $P_{D_s^{\pm}}$ are chosen to be non-relativistic Voigtian distributions (Voigt), because of the small number of floating shape parameters (three) and their good performance based on tests in simulated samples. A Voigtian distribution is the convolution of a Breit-Wigner distribution with a Gaussian (Gauss) distribution [48]. Since the $D^{\pm}$ and $D_s^{\pm}$ mesons have negligible natural widths, the detector resolution is absorbed by the shape parameters of both the Breit-Wigner distribution and the Gaussian distribution. The background contribution P_{Bkg}, originating mainly from combinatorics, is extracted using a normalised quadratic exponential distribution. Using RooFit [49], the extended unbinned maximum likelihood $\mathcal{L}(m)$ of the combined fit function is implemented as the following:

$$
\begin{aligned}
\mathcal{L}(m) &= \frac{\mathrm{e}^{-(S_{D^{\pm}}+S_{D_s^{\pm}}+B)}}{n!} \prod \Big[S_{D^{\pm}} P_{D^{\pm}}(m) + S_{D_s^{\pm}} P_{D_s^{\pm}}(m) + B P_{\mathrm{Bkg}}(m)\Big] \times \mathcal{G}(\Delta), \\
P_{D^{\pm}}(m) &= \mathrm{Voigt}(m; m_{D^{\pm}}, \gamma_{D^{\pm}}, \sigma_{D^{\pm}}), \\
P_{D_s^{\pm}}(m) &= \mathrm{Voigt}(m; m_{D_s^{\pm}}, \gamma_{D_s^{\pm}}, \sigma_{D_s^{\pm}}), \\
P_{\mathrm{Bkg}}(m) &= A_{\mathrm{norm}} \cdot \mathrm{e}^{(c_1 m + c_2 m^2)}, \\
\mathcal{G}(\Delta) &= \mathrm{Gauss}(\Delta; \mu_{\Delta}, \sigma_{\Delta}),
\end{aligned}
\tag{5.1}
$$

where A_{norm} is the normalisation factor of the quadratic exponential distribution, and $S_{D^{\pm}}$, $S_{D_s^{\pm}}$ and B are the yields of $D^{\pm}$ mesons, $D_s^{\pm}$ mesons and background, respectively. The

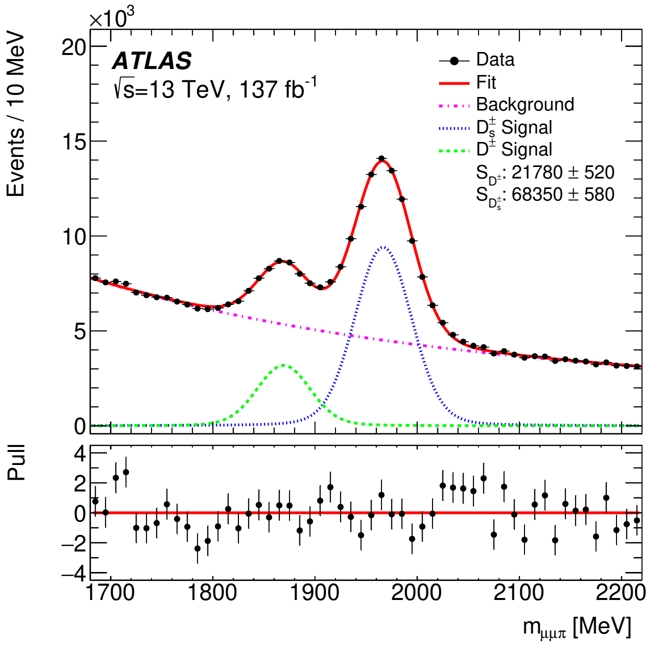

Figure 1. Invariant mass distribution of the di-muon-plus-track candidates. The unbinned fit according to eq. (5.1) is shown as a solid line, with the signal components for the $D^{\pm}$ and $D_s^{\pm}$ resonance fit presented as dashed and dotted lines, respectively; the background-only contribution is shown as a dash-dotted line. The signal yields extracted are also shown with corresponding statistical uncertainties. The lower panel shows the pull distribution.

Voigtian distributions of the $D^{\pm}$ and $D_s^{\pm}$ mesons are parameterised by the mean parameters $m_{D^{\pm}}$ and $m_{D_s^{\pm}}$, while $\gamma_{D^{\pm}}$ and $\gamma_{D_s^{\pm}}$ are the widths of the Breit-Wigner distributions and the widths of the Gaussian distributions are $\sigma_{D^{\pm}}$ and $\sigma_{D_s^{\pm}}$. The parameter c_1 is the linear rate parameter as in a simple exponential distribution, while the parameter c_2 is the quadratic part that is multiplied by m^2. The mass difference Δ is defined as $m_{D_s^{\pm}} - m_{D^{\pm}}$, which is constrained to be close to the world average mass difference μ_{Δ} [3] of the two D mesons by using an additional Gaussian constraint $\mathcal{G}(\Delta)$ with mean μ_{Δ} and width σ_{Δ}.

In the model, the parameters of interest are the yields $S_{D^{\pm}}$ and $S_{D_s^{\pm}}$, while the other parameters that determine the background model and the signal shape are regarded as nuisance parameters. To improve the stability of the fit model, particularly in bins with low numbers of candidates, fits are performed to the MC simulated events to fix some of the nuisance parameters, including $\gamma_{D^{\pm}}$ and $\gamma_{D_s^{\pm}}$. The unbinned maximum-likelihood fit to the mass spectrum is presented in figure 1; for each data point, the pull is defined as the difference between the data and the fitted model divided by the statistical uncertainty in the data point. It can be observed in the figure and in the fits to different kinematic regions in section 5.3 that this approach achieves compatibility with the observed data while reducing the number of fit parameters.

JHEP07(2025)086

5.2 Lifetime fit model

This section describes the extraction of prompt and non-prompt lifetime templates from the MC simulation, together with a template fit to the data to estimate the contribution from non-prompt processes. To quantify the proportion of non-prompt processes, the non-prompt fraction f_{NP} is defined as the yield of non-prompt signal divided by the total signal yield. The two production mechanisms mainly differ in terms of the average decay distance from the PV. From the reconstructed vertex position, the pseudo-proper-lifetime (hereinafter referred to as lifetime) τ of the $\mu\mu\pi$ candidates is calculated as:

$$\tau = \frac{m_{\mu\mu\pi} L_{xy}}{p_{\mathrm{T}}}. \tag{5.2}$$

Because of the relatively long lifetime of $D^{\pm}$ ($D_s^{\pm}$) mesons, they can travel for approximately 1 ps (0.5 ps) before they decay into a ϕ meson and a pion. The prompt contribution therefore includes an exponential distribution (Exp) to describe the physical exponential decay of the particle, which is convolved with a Gaussian distribution (Gauss) and an error function (Erf) to account for the detector resolution and the turn-on effect at low lifetime. The turn-on effect describes the transition in efficiency from zero to a constant at low lifetime, which is mainly due to the requirement on the significance of L_{xy}.

For the non-prompt production mode, the B meson, which has a typical lifetime of 1.5 ps, can travel a few millimeters before it decays into a $D^{\pm}/D_s^{\pm}$ meson. The non-prompt contribution therefore includes one exponential distribution to account for the cascade decay of the B meson, and another exponential distribution to account for the lifetime of the $D^{\pm}/D_s^{\pm}$ mesons. As for the prompt contribution, the distribution is also convolved with a Gaussian distribution and an error function to account for detector effects.

The templates for the non-prompt contribution $P_{b\bar{b}}(\tau)$ and the template for the prompt contribution $P_{c\bar{c}}(\tau)$ are defined as follows:

$$\begin{aligned} P_{b\bar{b}}(\tau) &= \mathrm{Exp}(\tau;\tau_D^{b\bar{b}}) * \mathrm{Exp}(\tau;\tau_B^{b\bar{b}}) * \mathrm{Gauss}(\tau;\mu^{b\bar{b}},\sigma_{\mathrm{res}}^{b\bar{b}}) * \mathrm{Erf}(\tau;\tau_{\text{turn-on}}^{b\bar{b}},\beta^{b\bar{b}}), \\ P_{c\bar{c}}(\tau) &= \mathrm{Exp}(\tau;\tau_D^{c\bar{c}}) * \mathrm{Gauss}(\tau;\mu^{c\bar{c}},\sigma_{\mathrm{res}}^{c\bar{c}}) * \mathrm{Erf}(\tau;\tau_{\text{turn-on}}^{c\bar{c}},\beta^{c\bar{c}}). \end{aligned} \tag{5.3}$$

Here the asterisk sign $*$ indicates the linear convolution between the functions, τ is the lifetime of the secondary vertex, $\tau_D^{b\bar{b}}$ and $\tau_D^{c\bar{c}}$ are the lifetime components of the $D^{\pm}/D_s^{\pm}$ meson, $\tau_B^{b\bar{b}}$ is the lifetime component of the B meson for the non-prompt decay, $\mu^{b\bar{b}}$ and $\mu^{c\bar{c}}$ represent a constant shift in lifetime due to detector bias, $\sigma_{\mathrm{res}}^{b\bar{b}}$ and $\sigma_{\mathrm{res}}^{c\bar{c}}$ describe the smearing due to detector resolution, $\tau_{\text{turn-on}}^{b\bar{b}}$ and $\tau_{\text{turn-on}}^{c\bar{c}}$ represent a constant shift in lifetime due to the turn-on effect, and $\beta^{b\bar{b}}$ and $\beta^{c\bar{c}}$ are multiplicative factors applied to the lifetime that determine the sharpness of the turn-on effect. These functions are fitted to the prompt and non-prompt MC simulated events separately to extract the templates, and the parameters are fixed before extracting the non-prompt fraction from data.

Before performing a lifetime fit to the data using the MC templates, the signal distribution must be extracted from data by removing the background contribution. Invariant mass fits (as described in section 5.1) are performed in bins of the lifetime, τ, allowing the signal yield N_i and its uncertainty σ_i to be extracted in each lifetime interval i for the data. A minimum χ^2 fit is performed on the extracted signal distribution using the prompt and

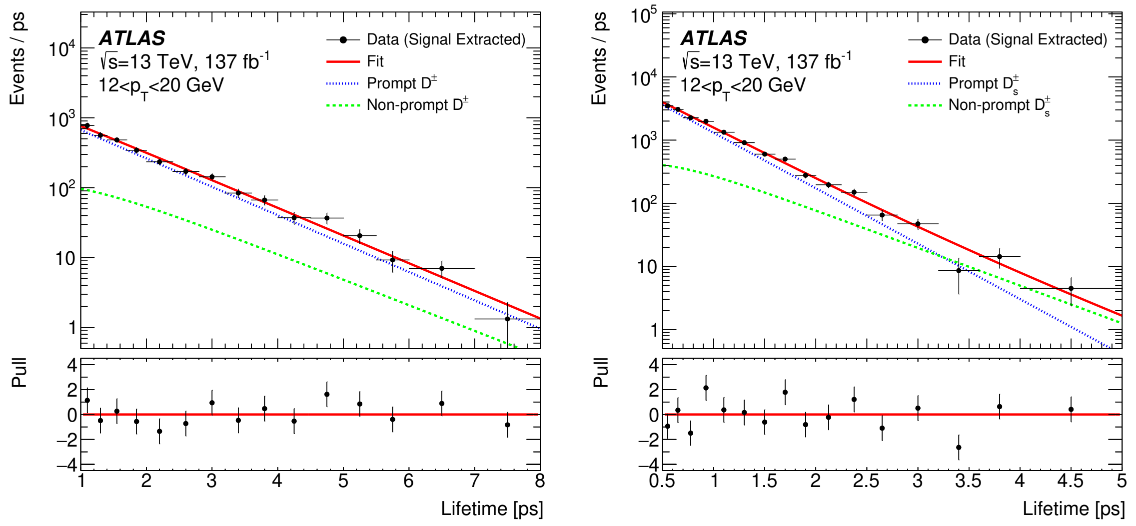

(a) (b)

Figure 2. Template fits to the lifetime distribution extracted from data for (a) $D^{\pm}$ and (b) $D_s^{\pm}$ mesons in the range of $12 < p_{\mathrm{T}} < 20$ GeV. The prompt and non-prompt contributions are presented as dotted and dashed lines, respectively; the combined fits are shown as solid lines. The bin sizes are variable, and the data points are drawn at the bin centres. The lower panels show the pull distributions.

non-prompt lifetime templates. Since the parameters of the individual MC templates are fixed, the only fit parameter is the non-prompt fraction f_{NP}. With such an approach, the fits can extract yields up to lifetimes of 5.0 ps for the $D_s^{\pm}$ meson and 8.0 ps for the $D^{\pm}$ meson; beyond this, there are insufficient data to perform the fits. Because the signal yields are extracted in finite bins of lifetime, the sharply rising slope at low lifetime cannot be reliably extracted; therefore, the region with low lifetime is excluded from the fit. For the $D^{\pm}$ meson, the region with lifetime less than 1.0 ps is excluded; for the $D_s^{\pm}$ meson, the region with lifetime less than 0.5 ps is excluded.

The procedure is applied separately for $D^{\pm}$ and $D_s^{\pm}$ mesons across three bins of p_{T}; in each bin of p_{T}, the individual templates and the combined models are all fitted separately. The bins are defined to capture the falling shape of f_{NP}, while ensuring enough data are present in each bin. The bin boundaries in p_{T} are [12, 20, 30, 100] GeV. Figure 2 shows the extracted signal from data and the fits with the combined model for the first p_{T} region. The χ^2 divided by the number of degrees of freedom of the fits ranges from 0.6 to 1.5, showing a good agreement between the model and the data.

Figure 3 shows the extracted non-prompt fraction and the corresponding statistical uncertainties for both $D^{\pm}$ and $D_s^{\pm}$ in bins of p_{T}. The statistical uncertainties for $D^{\pm}$ mesons are larger than those for $D_s^{\pm}$ mesons. This is due to the lower yield and the longer lifetime of the $D^{\pm}$ meson, which reduces the discriminating power of the fit because of the increased similarity between the prompt and non-prompt shapes.

The non-prompt fraction is then used to construct the weights for the MC simulated events, such that the non-prompt contribution in data is matched in the MC simulated events. The uncertainties in the non-prompt fractions are relatively large; therefore, no

JHEP07(2025)086

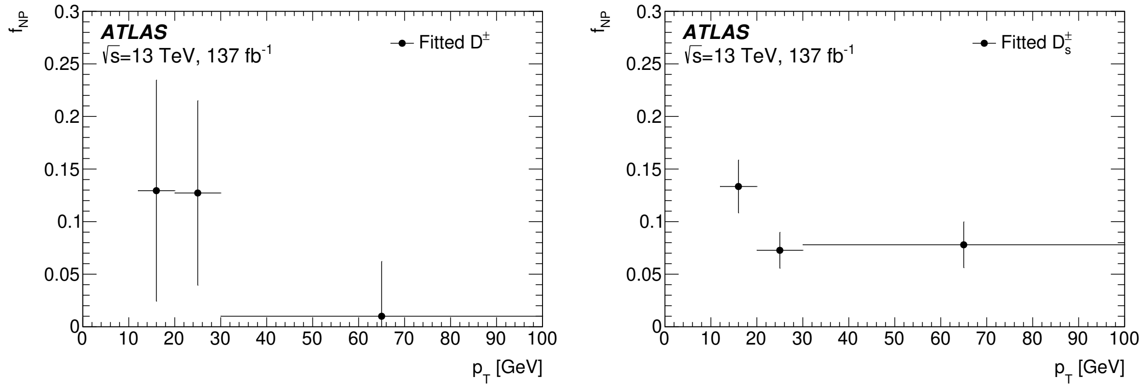

(a) (b)

Figure 3. Estimated non-prompt fraction of (a) $D^{\pm}$ and (b) $D_s^{\pm}$ meson production as a function of p_{T}, in the fiducial volume defined by $12 < p_{\mathrm{T}} < 100$ GeV and $|\eta| < 2.5$. Only the statistical uncertainties are shown.

interpretation or comparison is made with theoretical predictions. However, the extracted uncertainties in the non-prompt fractions allow the systematic uncertainties for the two production mechanisms to be evaluated.

5.3 Cross-section measurement

The differential cross-section is measured in the fiducial volume defined by $12 < p_{\mathrm{T}} < 100$ GeV and $|\eta| < 2.5$ for $D^{\pm}$ and $D_s^{\pm}$ mesons, in nine bins of p_{T} and five bins in $|\eta|$. To obtain the differential cross-section in a given bin, the yields of $D^{\pm}$ and $D_s^{\pm}$ mesons in the bin are obtained from a fit to the triplet mass $m_{\mu\mu\pi}$, as described in section 5.1. Figures 4 and 5 show the examples of the invariant mass fits in two regions of $|\eta|$ and p_{T}, respectively.

For each bin in p_{T} (denoted by i) and each bin in $|\eta|$ (denoted by j), the yield obtained is then divided by the overall efficiency, bin width, branching ratio $\mathcal{B}$, and the integrated luminosity to evaluate the differential production cross-section. The differential cross-sections in p_{T} and $|\eta|$ are given by the following equations:

$$\begin{aligned}\left.\frac{\mathrm{d}\sigma}{\mathrm{d}p_{\mathrm{T}}}\right|_i &= \frac{S^i_{D^{\pm}/D_s^{\pm}}}{\int \mathcal{L}\mathrm{d}t \times C^i \times \mathcal{B}(D^{\pm}/D_s^{\pm} \to \phi(\mu\mu)\pi^{\pm}) \times \Delta^i p_{\mathrm{T}}},\\ \left.\frac{\mathrm{d}\sigma}{\mathrm{d}|\eta|}\right|_j &= \frac{S^j_{D^{\pm}/D_s^{\pm}}}{\int \mathcal{L}\mathrm{d}t \times C^j \times \mathcal{B}(D^{\pm}/D_s^{\pm} \to \phi(\mu\mu)\pi^{\pm}) \times \Delta^j |\eta|},\end{aligned} \tag{5.4}$$

where $S^i_{D^{\pm}/D_s^{\pm}}$ and $S^j_{D^{\pm}/D_s^{\pm}}$ are the yields of $D^{\pm}$ and $D_s^{\pm}$ signals extracted in bins of p_{T} and $|\eta|$, $\Delta^i p_{\mathrm{T}}$ is the bin width in p_{T}, and $\Delta^j|\eta|$ is the bin width in $|\eta|$. The integrated luminosity, $\int \mathcal{L}\mathrm{d}t$, is 137 fb^{-1} [24]. The correction factors C^i and C^j account for the reconstruction and selection efficiency and acceptance, which are derived bin-by-bin in p_{T} and $|\eta|$, respectively, using MC simulated events.

The branching ratio of the $D_s^{\pm}$ decay chain is given by:

$$\mathcal{B}(D_s^{\pm} \to \phi(\mu\mu)\pi^{\pm}) = \frac{\mathcal{B}(D_s^{\pm} \to \phi(K^+K^-)\pi^{\pm})}{\mathcal{B}(\phi \to K^+K^-)} \times \mathcal{B}(\phi \to \mu\mu), \tag{5.5}$$

JHEP07(2025)086

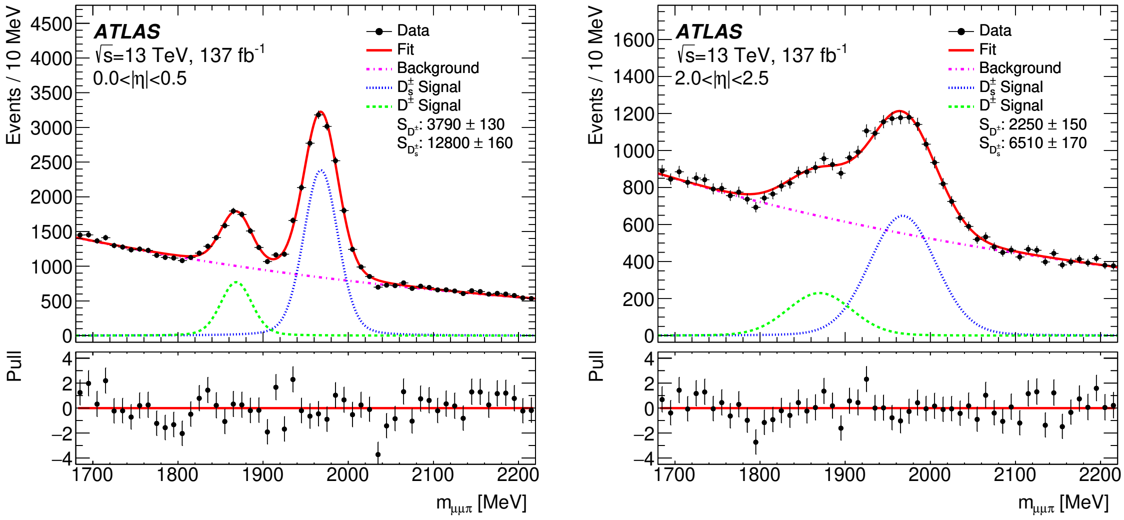

(a) (b)

Figure 4. Examples of fits to the distribution of invariant mass $m_{\mu\mu\pi}$ in regions of (a) $0.0 < |\eta| < 0.5$ and (b) $2.0 < |\eta| < 2.5$. The unbinned fits according to eq. (5.1) are shown as solid lines, with the signal components for the $D^{\pm}$ and $D_s^{\pm}$ resonance fit presented as dashed and dotted lines, respectively; the background-only contributions are shown as dash-dotted lines. The signal yields extracted are also shown with corresponding statistical uncertainties. The lower panels show the pull distributions.

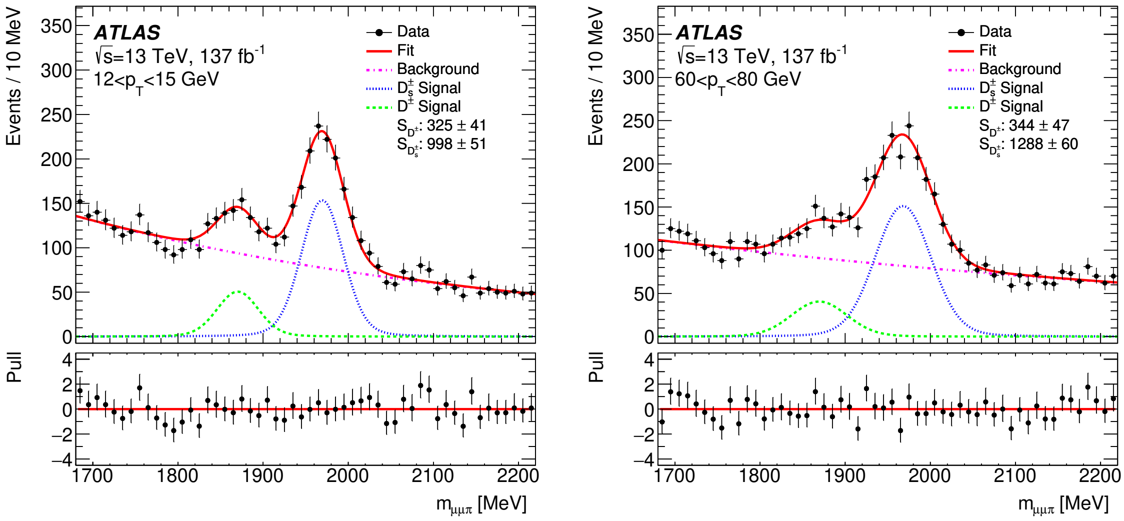

(a) (b)

Figure 5. Examples of fits to the distribution of invariant mass $m_{\mu\mu\pi}$ in regions of (a) $12 < p_{\mathrm{T}} < 15$ GeV and (b) $60 < p_{\mathrm{T}} < 80$ GeV. The unbinned fits according to eq. (5.1) are shown as solid lines, with the signal components for the $D^{\pm}$ and $D_s^{\pm}$ resonance fit presented as dashed and dotted lines, respectively; the background-only contributions are shown as dash-dotted lines. The signal yields extracted are also shown with corresponding statistical uncertainties. The lower panels show the pull distributions.

JHEP07(2025)086

as the uncertainties of the world average branching ratios of the $D_s^{\pm} \to \phi(K^+K^-)\pi^{\pm}$ and $\phi \to K^+K^-$ processes combined are better than the branching ratio of $D_s^{\pm} \to \phi\pi^{\pm}$ [3]. For the $D^{\pm}$ meson, the branching ratio is taken as the product of the branching ratios of the $D^{\pm} \to \phi\pi^{\pm}$ and $\phi \to \mu\mu$ processes [3].

The cross-section in the fiducial volume is determined by summing over the bins i of the differential cross-section as a function of p_{T}, according to:

$$\sigma_{\text{fiducial}} = \sum_i \left.\frac{\mathrm{d}\sigma}{\mathrm{d}p_{\mathrm{T}}}\right|_i \Delta^i p_{\mathrm{T}}. \tag{5.6}$$

Summing over the differential cross-section in bins of $|\eta|$ is found to give a consistent result when compared to summing over p_{T}.

To facilitate the use of the result as a normalisation for other studies and as a comparison with previous measurements, different fiducial volumes are considered. The lower p_{T} boundary of 12 GeV corresponds to the lowest p_{T} reach; the p_{T} boundaries of 15 and 20 GeV are also considered. The p_{T} boundary of 15 GeV provides a p_{T} range that is above the trigger efficiency plateau to reduce the muon and trigger uncertainties; the p_{T} boundary of 20 GeV provides a p_{T} range compatible with the previous ATLAS measurements [16].

6 Systematic uncertainties

The uncertainties in the signal yields, acceptance correction factors, integrated luminosity, and the decay branching ratios are propagated linearly to the differential and thus to the integrated fiducial cross-sections according to eq. (5.4). The systematic uncertainties can be categorised into detector effects, production modelling, branching ratio, MC simulated data sample size and signal extraction.

The systematic uncertainties due to detector effects are as follows:

Muon: The uncertainties on the muon reconstruction were evaluated in dedicated studies using $J/\psi \to \mu\mu$ and $Z \to \mu\mu$ events [45, 50]. The muon reconstruction and identification efficiency uncertainties [45] affect the acceptance correction factors in eq. (5.4), while those on muon momentum calibration [50] can also cause bin migrations in the differential measurements.

Tracking: The uncertainty in the track reconstruction efficiency arises primarily from the limited knowledge of the ID material description used in MC simulation. Uncertainties in track momentum and impact parameter calibration are also accounted for in vertex fitting and selection [51].

Pile-up: Pile-up refers to the number of simultaneous pp collisions in the same event. Weights are applied to MC simulation to make the pile-up distribution match that in data and are varied according to its uncertainty.

Trigger: The trigger efficiencies are measured in data using $J/\psi \to \mu\mu$ events following the procedure described in ref. [52]. The MC simulated samples are corrected to reproduce the measured efficiencies, and the uncertainty of the measurement is accounted for as a systematic uncertainty.

JHEP07(2025)086

Luminosity: The uncertainty in the integrated luminosity of the combined data sample from 2016, 2017, and 2018 is 0.84%, using the same methodology as in ref. [24], and obtained using the LUCID-2 detector [20] for the primary luminosity measurements, complemented by measurements using the ID and calorimeters.

The systematic uncertainties due to the modelling of $D^{\pm}$ and $D_s^{\pm}$ meson production are as follows:

Non-prompt: To correct for the MC modelling of the non-prompt $D^{\pm}$ and $D_s^{\pm}$ meson production fractions, the procedure described in section 5.2 is used. The uncertainties on the non-prompt fractions are propagated to the yields of the simulated samples, and further propagated to the acceptance correction factors.

Kinematics: The MC simulated p_{T} spectra of $D^{\pm}$ and $D_s^{\pm}$ meson production are corrected to match the distribution extracted from data. The statistical uncertainties in the data spectra are propagated to the acceptance correction factors using this procedure. The uncertainties due to the $|\eta|$ spectra modelling are found to be negligible, while those of the p_{T} spectra have a small effect when propagated to the differential cross-section measurements in $|\eta|$.

The remaining systematic uncertainties are as follows:

Branching ratio (BR): The uncertainties in the branching ratios are taken from ref. [3]. For the $D^{\pm}$ meson, the total uncertainty in the decay chain is 7.2%, while that of the $D_s^{\pm}$ meson is 7.3%.

MC size: The statistical uncertainty due to limited size of MC simulated signal samples is propagated to the measurement results via the acceptance correction factors.

Fit model (signal and background): The fit model systematic uncertainties can be separated into contributions from the signal model and the background model. By varying the models, the difference in yield is taken as a systematic uncertainty. MC pseudo data are generated according to the distribution obtained from data, according to Poisson fluctuations; fits with alternative models are then applied to the pseudo data. For the signal model, the Bukin model [53] and triple Gaussian models are chosen as alternatives. For the background model, a simple exponential model is taken as the alternative. By repeatedly fitting the nominal models and the alternative models to the pseudo data, the distributions of the yield estimators are obtained. The mean yield differences between the nominal model and the alternative models are taken as the systematic uncertainties. The background model systematic uncertainty is also checked to cover the effects of possible contributions from partially reconstructed D meson decays, such as $D^{\pm}/D_s^{\pm} \to \phi\pi^{\pm}\pi^{0}$ decays. Because of the limited amount of data, these uncertainties are evaluated in a single bin above $p_{\mathrm{T}} = 40\,\mathrm{GeV}$.

The uncertainties above are evaluated in bins of p_{T} and $|\eta|$, except for the uncertainties in the luminosity and branching ratios. Figures 6 and 7 show the systematic uncertainty profiles of $D^{\pm}$ and $D_s^{\pm}$ mesons in bins of p_{T} and $|\eta|$.

JHEP07(2025)086

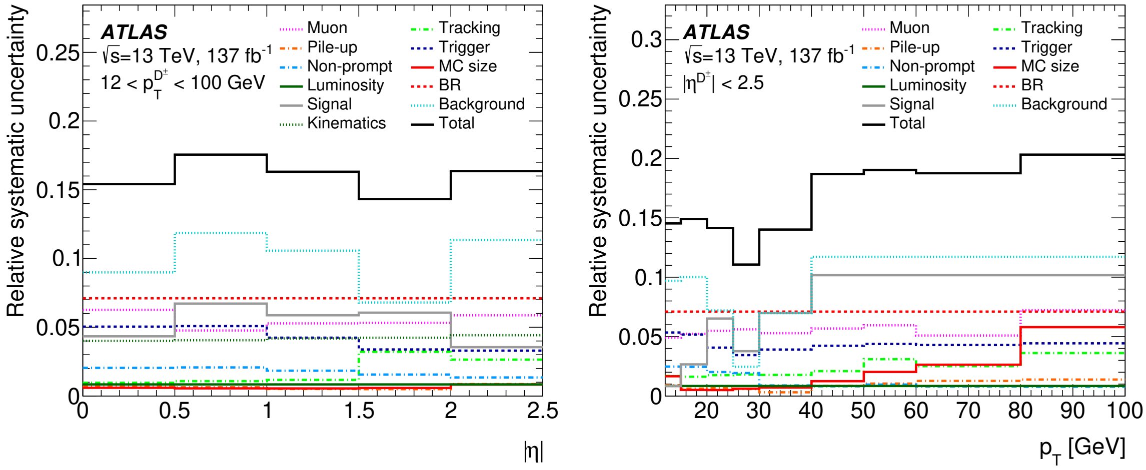

(a) (b)

Figure 6. Relative systematic uncertainty profile of the differential cross-sections for $D^{\pm}$ mesons, in bins of (a) $|\eta|$ and (b) p_{T}. The systematic uncertainties shown are also combined in quadrature (upper solid line).

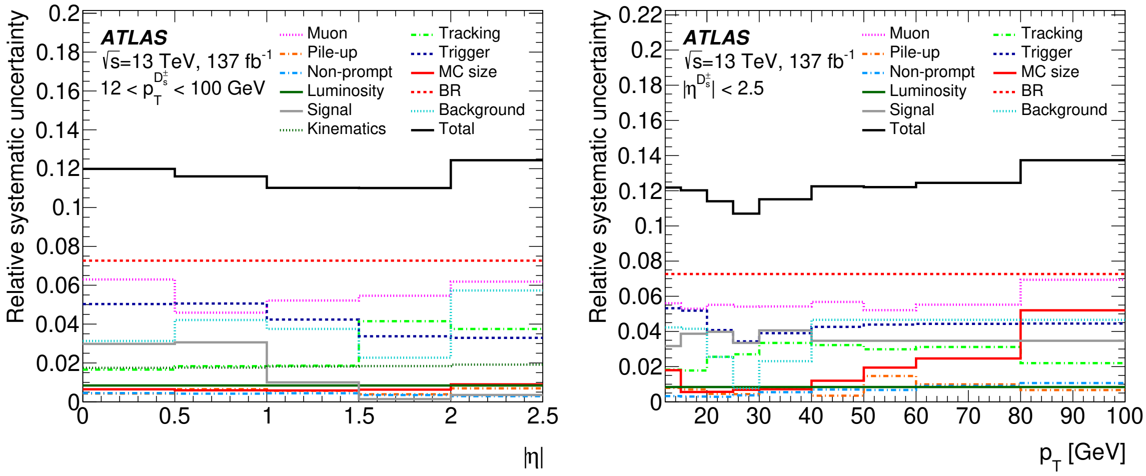

(a) (b)

Figure 7. Relative systematic uncertainty profile of the differential cross-sections for $D_s^{\pm}$ mesons, in bins of (a) $|\eta|$ and (b) p_{T}. The systematic uncertainties shown are also combined in quadrature (upper solid line).

For the $D_s^{\pm}$ measurement, the largest systematic uncertainty contributions arise from the decay branching ratios, followed by the trigger uncertainty and background modelling uncertainty. For the $D^{\pm}$ cross-section, the background modelling uncertainty dominates in most of the phase space. The combined systematic uncertainty is mainly in the range of 10%–14% for the $D_s^{\pm}$ and 15%–20% for the $D^{\pm}$ due to the latter being more sensitive to the choice of background model.

JHEP07(2025)086

Range	Differential cross-section [µb] Data	GM-VFNS	FONLL
	$\frac{d\sigma}{d\|\eta\|} \pm \delta_{\text{stat}} \pm \delta_{\text{syst}} \pm \delta_{\text{BR}}$	$\frac{d\sigma}{d\|\eta\|} \pm \delta_{\text{theory}}$	$\frac{d\sigma}{d\|\eta\|} \pm \delta_{\text{theory}}$
$0.0 < \|\eta\| < 0.5$	$5.15 \pm 0.18 \pm 0.71 \pm 0.37$	$6.4^{+1.3}_{-1.1}$	$4.7^{+1.2}_{-0.9}$
$0.5 < \|\eta\| < 1.0$	$5.84 \pm 0.19 \pm 0.93 \pm 0.41$	$6.2^{+1.3}_{-1.0}$	$4.5^{+1.2}_{-0.9}$
$1.0 < \|\eta\| < 1.5$	$4.96 \pm 0.22 \pm 0.73 \pm 0.35$	$5.8^{+1.2}_{-1.0}$	$4.2^{+1.1}_{-0.8}$
$1.5 < \|\eta\| < 2.0$	$3.62 \pm 0.18 \pm 0.43 \pm 0.26$	$5.3^{+1.1}_{-0.9}$	$3.8^{+1.0}_{-0.7}$
$2.0 < \|\eta\| < 2.5$	$3.33 \pm 0.23 \pm 0.49 \pm 0.24$	$4.5^{+0.9}_{-0.7}$	$3.2^{+0.9}_{-0.6}$

Table 2. The measured differential cross-sections and the predictions from GM-VFNS and FONLL calculations for the $D^{\pm}$ meson in bins of $|\eta|$ for $12 < p_{\mathrm{T}} < 100\,\text{GeV}$. The statistical, systematic (excluding branching ratio) and branching ratio uncertainties are shown separately for data, while the total theoretical uncertainties are shown for GM-VFNS and FONLL.

7 Results

The values of the measured differential cross-sections and the theory predictions are shown in tables 2–5 for $D^{\pm}$ and $D_s^{\pm}$ mesons; they are also shown in figure 8. The fiducial cross-section is summarised in table 6, including the theory predictions available.

JHEP07(2025)086

Range [GeV]	Differential cross-section [pb/GeV] Data	GM-VFNS	FONLL
	$\frac{d\sigma}{dp_T} \pm \delta_{stat} \pm \delta_{syst} \pm \delta_{BR}$	$\frac{d\sigma}{dp_T} \pm \delta_{theory}$	$\frac{d\sigma}{dp_T} \pm \delta_{theory}$
$12 < p_T < 15$	$(1.80 \pm 0.23 \pm 0.22 \pm 0.13) \times 10^6$	$2.45^{+0.58}_{-0.44} \times 10^6$	$1.82^{+0.54}_{-0.38} \times 10^6$
$15 < p_T < 20$	$(7.0 \pm 0.3 \pm 0.9 \pm 0.5) \times 10^5$	$8.5^{+1.7}_{-1.4} \times 10^5$	$6.1^{+1.5}_{-1.1} \times 10^5$
$20 < p_T < 25$	$(2.10 \pm 0.08 \pm 0.25 \pm 0.15) \times 10^5$	$2.76^{+0.44}_{-0.39} \times 10^5$	$1.90^{+0.39}_{-0.31} \times 10^5$
$25 < p_T < 30$	$(9.2 \pm 0.4 \pm 0.8 \pm 0.7) \times 10^4$	$1.10^{+0.15}_{-0.14} \times 10^5$	$7.3^{+1.3}_{-1.1} \times 10^4$
$30 < p_T < 40$	$(2.86 \pm 0.12 \pm 0.34 \pm 0.20) \times 10^4$	$3.75^{+0.43}_{-0.44} \times 10^4$	$2.44^{+0.38}_{-0.33} \times 10^4$
$40 < p_T < 50$	$(8.7 \pm 0.5 \pm 1.5 \pm 0.6) \times 10^3$	$1.08^{+0.10}_{-0.11} \times 10^4$	$6.8^{+0.9}_{-0.8} \times 10^3$
$50 < p_T < 60$	$(2.45 \pm 0.31 \pm 0.43 \pm 0.17) \times 10^3$	$3.89^{+0.30}_{-0.37} \times 10^3$	$2.41^{+0.29}_{-0.28} \times 10^3$
$60 < p_T < 80$	$(8.9 \pm 1.2 \pm 1.5 \pm 0.6) \times 10^2$	$1.21^{+0.08}_{-0.10} \times 10^3$	$7.3^{+0.8}_{-0.8} \times 10^2$
$80 < p_T < 100$	$(1.78 \pm 0.64 \pm 0.34 \pm 0.13) \times 10^2$	$3.08^{+0.16}_{-0.24} \times 10^2$	$1.81^{+0.19}_{-0.18} \times 10^2$

Table 3. The measured differential cross-sections and the predictions from GM-VFNS and FONLL calculations for the $D^{\pm}$ meson in bins of p_T for $|\eta| < 2.5$. The statistical, systematic (excluding branching ratio) and branching ratio uncertainties are shown separately for data, while the total theoretical uncertainties are shown for GM-VFNS and FONLL.

Range	Differential cross-section [µb] Data	GM-VFNS
	$\frac{d\sigma}{d\|\eta\|} \pm \delta_{stat} \pm \delta_{syst} \pm \delta_{BR}$	$\frac{d\sigma}{d\|\eta\|} \pm \delta_{theory}$
$0.0 < \|\eta\| < 0.5$	$2.51 \pm 0.03 \pm 0.24 \pm 0.18$	$2.69^{+0.56}_{-0.45}$
$0.5 < \|\eta\| < 1.0$	$2.61 \pm 0.03 \pm 0.23 \pm 0.19$	$2.62^{+0.55}_{-0.44}$
$1.0 < \|\eta\| < 1.5$	$2.23 \pm 0.04 \pm 0.18 \pm 0.16$	$2.46^{+0.51}_{-0.41}$
$1.5 < \|\eta\| < 2.0$	$1.79 \pm 0.03 \pm 0.13 \pm 0.13$	$2.22^{+0.46}_{-0.37}$
$2.0 < \|\eta\| < 2.5$	$1.44 \pm 0.04 \pm 0.13 \pm 0.10$	$1.90^{+0.39}_{-0.32}$

Table 4. The measured differential cross-sections and the predictions from the GM-VFNS calculation for the $D_s^{\pm}$ meson in bins of $|\eta|$ for $12 < p_T < 100$ GeV. The statistical, systematic (excluding branching ratio) and branching ratio uncertainties are shown separately for data, while the total theoretical uncertainties are shown for GM-VFNS.

JHEP07(2025)086

Range [GeV]	Differential cross-section [pb/GeV] Data	GM-VFNS
	$\frac{d\sigma}{dp_T} \pm \delta_{stat} \pm \delta_{syst} \pm \delta_{BR}$	$\frac{d\sigma}{dp_T} \pm \delta_{theory}$
$12 < p_T < 15$	$(8.5 \pm 0.4 \pm 0.8 \pm 0.6) \times 10^5$	$1.02^{+0.24}_{-0.18} \times 10^6$
$15 < p_T < 20$	$(3.04 \pm 0.06 \pm 0.29 \pm 0.22) \times 10^5$	$3.62^{+0.71}_{-0.59} \times 10^5$
$20 < p_T < 25$	$(1.01 \pm 0.01 \pm 0.08 \pm 0.07) \times 10^5$	$1.19^{+0.19}_{-0.17} \times 10^5$
$25 < p_T < 30$	$(4.20 \pm 0.06 \pm 0.31 \pm 0.31) \times 10^4$	$4.75^{+0.65}_{-0.62} \times 10^4$
$30 < p_T < 40$	$(1.45 \pm 0.02 \pm 0.12 \pm 0.11) \times 10^4$	$1.64^{+0.19}_{-0.19} \times 10^4$
$40 < p_T < 50$	$(3.82 \pm 0.09 \pm 0.36 \pm 0.28) \times 10^3$	$4.74^{+0.45}_{-0.50} \times 10^3$
$50 < p_T < 60$	$(1.38 \pm 0.05 \pm 0.13 \pm 0.10) \times 10^3$	$1.72^{+0.14}_{-0.17} \times 10^3$
$60 < p_T < 80$	$(4.55 \pm 0.21 \pm 0.44 \pm 0.33) \times 10^2$	$5.39^{+0.37}_{-0.47} \times 10^2$
$80 < p_T < 100$	$(8.1 \pm 0.9 \pm 0.9 \pm 0.6) \times 10^1$	$1.38^{+0.08}_{-0.11} \times 10^2$

Table 5. The measured differential cross-sections and the predictions from the GM-VFNS calculation for the $D_s^{\pm}$ meson in bins of p_T for $|\eta| < 2.5$. The statistical, systematic (excluding branching ratio) and branching ratio uncertainties are shown separately for data, while the total theoretical uncertainties are shown for GM-VFNS.

JHEP07(2025)086

Fiducial volume	$D^{\pm}$ inclusive fiducial cross-section at $\sqrt{s} = 13\,\text{TeV}$ [nb]		
	ATLAS	GM-VFNS	FONLL
	$\sigma \pm \delta_{\text{stat}} \pm \delta_{\text{syst}} \pm \delta_{\text{BR}}$	$\sigma \pm \delta_{\text{theory}}$	$\sigma \pm \delta_{\text{theory}}$
$12 < p_{\text{T}} < 100$ GeV, $\lvert\eta\rvert < 2.5$	$10\,800 \pm 900 \pm 1\,300 \pm 800$	$14\,100^{+2\,900}_{-2\,300}$	$10\,200^{+2\,300}_{-1\,700}$
$15 < p_{\text{T}} < 100$ GeV, $\lvert\eta\rvert < 2.5$	$5\,430 \pm 550 \pm 680 \pm 390$	$6\,800^{+1\,200}_{-1\,000}$	$4\,730^{+900}_{-700}$
$20 < p_{\text{T}} < 100$ GeV, $\lvert\eta\rvert < 2.5$	$1\,930 \pm 160 \pm 220 \pm 140$	$2\,480^{+350}_{-330}$	$1\,670^{+260}_{-220}$
	$D_s^{\pm}$ inclusive fiducial cross-section at $\sqrt{s} = 13\,\text{TeV}$ [nb]		
Fiducial volume	ATLAS	GM-VFNS	
	$\sigma \pm \delta_{\text{stat}} \pm \delta_{\text{syst}} \pm \delta_{\text{BR}}$	$\sigma \pm \delta_{\text{theory}}$	
$12 < p_{\text{T}} < 100$ GeV, $\lvert\eta\rvert < 2.5$	$5\,000 \pm 360 \pm 470 \pm 360$	$5\,900^{+1\,200}_{-1\,000}$	
$15 < p_{\text{T}} < 100$ GeV, $\lvert\eta\rvert < 2.5$	$2\,440 \pm 190 \pm 220 \pm 180$	$2\,880^{+510}_{-440}$	
$20 < p_{\text{T}} < 100$ GeV, $\lvert\eta\rvert < 2.5$	$920 \pm 60 \pm 80 \pm 70$	$1\,070^{+150}_{-140}$	

Table 6. Inclusive $D^{\pm}$ and $D_s^{\pm}$ meson production cross-sections in different fiducial volumes defined by $|\eta| < 2.5$ and different p_{T} regions. For the ATLAS measurements, the statistical, systematic (excluding branching ratio) and branching ratio uncertainties are shown separately; for the theoretical predictions, the total theoretical uncertainties are shown.

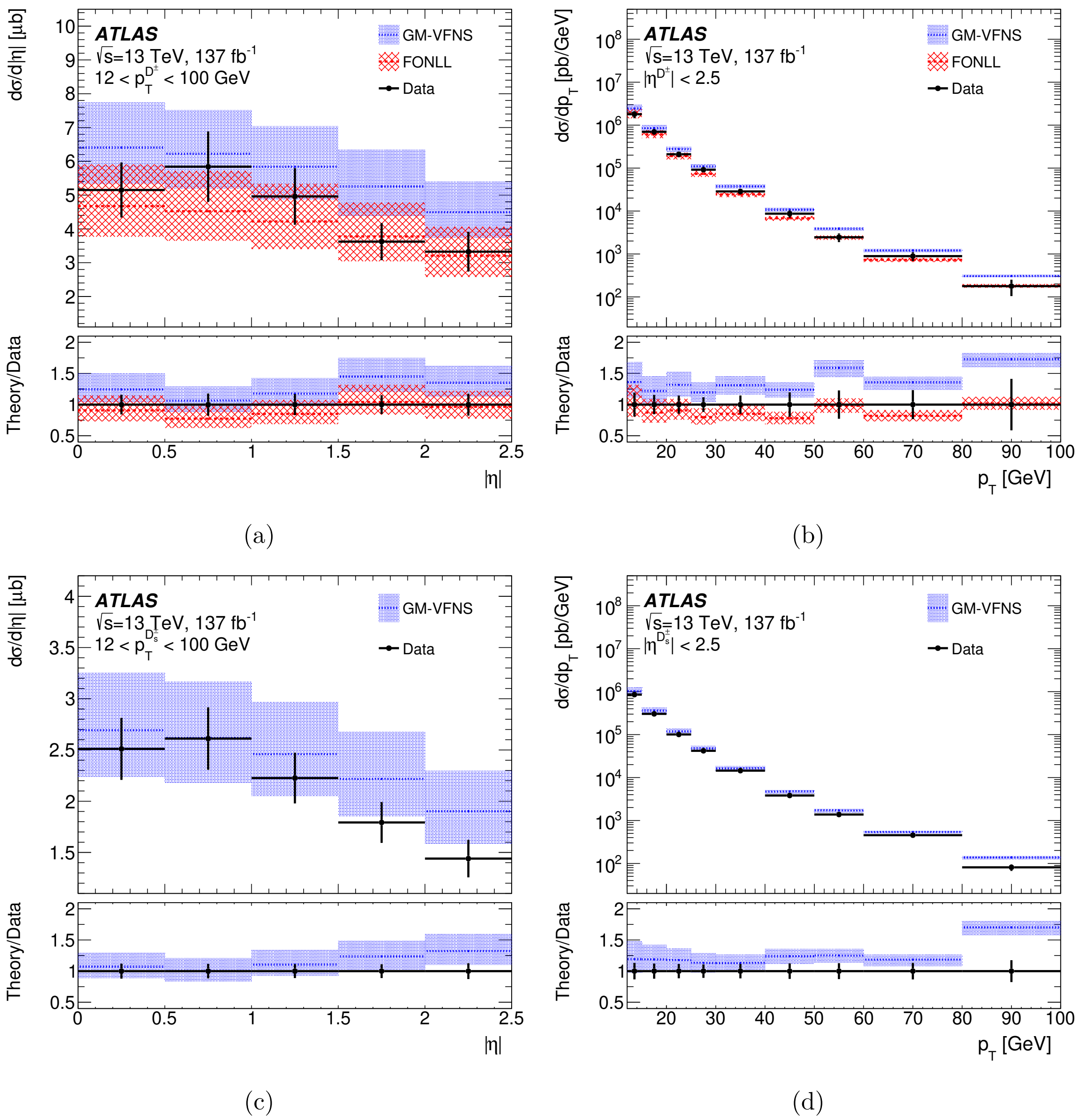

Figure 8. Differential cross-sections for $D^{\pm}$ mesons in bins of (a) $|\eta|$ and (b) p_{T}, and for $D_s^{\pm}$ mesons in bins of (c) $|\eta|$ and (d) p_{T}. The measured values with the statistical and systematic uncertainty are represented by the data points, while the theory predictions from GM-VFNS and FONLL are shown as dotted and dashed lines, respectively; the uncertainties on the theory predictions are represented by the hatched areas. The theory predictions are also divided by the measured values to obtain the ratios between the predictions and the measurements shown in the bottom panels.

For the $D^{\pm}$ meson, good agreement is observed at low p_{T} for both the GM-VFNS and FONLL predictions; the FONLL prediction is in general slightly lower than the measured differential cross-sections, while the GM-VFNS prediction is slightly higher. For higher p_{T}, the GM-VFNS prediction gives a larger value than the measured differential cross-section, while the FONLL prediction is still consistent with the measured values. When comparing in bins of $|\eta|$, good agreement is observed for both predictions, which is consistent with the observation in the low p_{T} bins.

For the $D_s^{\pm}$ meson, only the GM-VFNS prediction is available for comparison. Similar behaviour is observed; the GM-VFNS prediction gives a larger value than the measured differential cross-section for both $|\eta|$ and p_{T}, with a trend towards a larger deviation at higher p_{T}.

The results are compared with those measured with the pp collision data collected at a centre-of-mass energy of $\sqrt{s} = 7\,\mathrm{TeV}$ in 2010 [16]. Those measurements were performed using the $D^{\pm} \to K^{\mp}\pi^{\pm}\pi^{\pm}$ and $D_s^{\pm} \to \phi(K^+K^-)\pi^{\pm}$ decays for $|\eta| < 2.1$. To perform a consistent comparison, the difference between the fiducial volumes, particularly in $|\eta|$, must be taken into account. Since the differential cross-section in bins of $|\eta|$ is rather flat and well modelled by MC simulation, the ratio of the fiducial volume of $|\eta| < 2.1$ to $|\eta| < 2.5$ is derived from MC simulation with a negligible systematic uncertainty. Table 7 shows the comparison between the fiducial cross-sections measured at $\sqrt{s} = 13\,\mathrm{TeV}$ and $\sqrt{s} = 7\,\mathrm{TeV}$. For the $D_s^{\pm}$ meson, the measurement has a 12% uncertainty, which is an improvement over the 20% uncertainty in the previous measurement. For the $D^{\pm}$ meson, the measurement has a 14% uncertainty, which is larger than the previous uncertainty of 11%, mainly due to the background uncertainty driven by the low signal yield.

For both the ATLAS measurements, and the theory predictions, ratios between $\sqrt{s} = 7\,\mathrm{TeV}$ and $\sqrt{s} = 13\,\mathrm{TeV}$ are also computed. The statistical uncertainties in the two ATLAS measurements are independent because of the different data samples used; the systematic uncertainties are also assumed to be uncorrelated, because the two measurements used different decay channels with all main systematic uncertainty contributions being different. For FONLL and GM-VFNS, the uncertainties are assumed to be fully correlated between $\sqrt{s} = 7\,\mathrm{TeV}$ and $\sqrt{s} = 13\,\mathrm{TeV}$, as they are evaluated mainly from the variations of QCD scale uncertainties in a coherent way. In table 7, it can be seen that the ratios obtained by GM-VFNS and FONLL are both consistent with the data within the uncertainties. There is, however, a significant difference between the ratios predicted by GM-VFNS and FONLL.

JHEP07(2025)086

	$D^{\pm}$ inclusive fiducial cross-section [nb]		
	ATLAS	GM-VFNS	FONLL
	$\sigma \pm \delta_{\text{total}}$	$\sigma \pm \delta_{\text{theory}}$	$\sigma \pm \delta_{\text{theory}}$
$\sqrt{s} = 13\,\text{TeV}$	$1\,690 \pm 270$	$2\,200^{+310}_{-290}$	$1\,480^{+230}_{-190}$
$\sqrt{s} = 7\,\text{TeV}$	888 ± 97	980^{+120}_{-150}	620^{+100}_{-80}
Ratio (13 TeV/7 TeV)	1.9 ± 0.4	2.24 ± 0.04	2.38 ± 0.01
	$D_s^{\pm}$ inclusive fiducial cross-section [nb]		
	ATLAS	GM-VFNS	
	$\sigma \pm \delta_{\text{total}}$	$\sigma \pm \delta_{\text{theory}}$	
$\sqrt{s} = 13\,\text{TeV}$	810 ± 100	950^{+140}_{-130}	
$\sqrt{s} = 7\,\text{TeV}$	510 ± 100	470^{+56}_{-69}	
Ratio (13 TeV/7 TeV)	1.6 ± 0.4	2.02 ± 0.05	

Table 7. Inclusive $D^{\pm}$ and $D_s^{\pm}$ meson production cross-sections in a fiducial volume defined by $|\eta| < 2.1$ and $20 < p_{\text{T}} < 100$ GeV at $\sqrt{s} = 7\,\text{TeV}$ and $\sqrt{s} = 13\,\text{TeV}$. The total uncertainties are shown for both the ATLAS measurements and the theoretical predictions. The ratios of $\sqrt{s} = 13\,\text{TeV}$ values over $\sqrt{s} = 7\,\text{TeV}$ values are also computed by assuming the uncertainties are independent for different centre-of-mass energies.

8 Conclusions

The production of $D^{\pm}$ and $D_s^{\pm}$ charmed mesons is measured in the kinematic region $12 < p_{\text{T}} < 100\,\text{GeV}$ and $|\eta| < 2.5$ with the ATLAS detector at the LHC using $137\,\text{fb}^{-1}$ of $\sqrt{s} = 13\,\text{TeV}$ pp collision data. The differential cross-sections in bins of p_{T} and $|\eta|$ for $D^{\pm}$ and $D_s^{\pm}$ meson production are determined and compared with the available NLO QCD predictions. The fiducial cross-sections for $D^{\pm}$ and $D_s^{\pm}$ meson production are also presented; the values are compared with the predictions and with the measurement at $\sqrt{s} = 7\,\text{TeV}$. For the $D_s^{\pm}$ meson, this is the first measurement of the differential cross-section reported by the ATLAS Collaboration, and the first time such a measurement has been reported up to transverse momenta of 100 GeV, providing a benchmark for theoretical calculations in a previously unexplored kinematic space. The obtained cross-sections are compared with the predictions from the GM-VFNS and FONLL calculations, and the results are mostly consistent within the uncertainties, with slight deviation towards high-p_{T} regions.

Acknowledgments

We thank CERN for the very successful operation of the LHC and its injectors, as well as the support staff at CERN and at our institutions worldwide without whom ATLAS could not be operated efficiently.

The crucial computing support from all WLCG partners is acknowledged gratefully, in particular from CERN, the ATLAS Tier-1 facilities at TRIUMF/SFU (Canada), NDGF (Denmark, Norway, Sweden), CC-IN2P3 (France), KIT/GridKA (Germany), INFN-CNAF (Italy), NL-T1 (Netherlands), PIC (Spain), RAL (U.K.) and BNL (U.S.A.), the Tier-2 facilities worldwide and large non-WLCG resource providers. Major contributors of computing resources are listed in ref. [54].

We gratefully acknowledge the support of ANPCyT, Argentina; YerPhI, Armenia; ARC, Australia; BMWFW and FWF, Austria; ANAS, Azerbaijan; CNPq and FAPESP, Brazil; NSERC, NRC and CFI, Canada; CERN; ANID, Chile; CAS, MOST and NSFC, China; Minciencias, Colombia; MEYS CR, Czech Republic; DNRF and DNSRC, Denmark; IN2P3-CNRS and CEA-DRF/IRFU, France; SRNSFG, Georgia; BMBF, HGF and MPG, Germany; GSRI, Greece; RGC and Hong Kong SAR, China; ISF and Benoziyo Center, Israel; INFN, Italy; MEXT and JSPS, Japan; CNRST, Morocco; NWO, Netherlands; RCN, Norway; MNiSW, Poland; FCT, Portugal; MNE/IFA, Romania; MSTDI, Serbia; MSSR, Slovakia; ARIS and MVZI, Slovenia; DSI/NRF, South Africa; MICIU/AEI, Spain; SRC and Wallenberg Foundation, Sweden; SERI, SNSF and Cantons of Bern and Geneva, Switzerland; NSTC, Taipei; TENMAK, Türkiye; STFC/UKRI, United Kingdom; DOE and NSF, United States of America.

Individual groups and members have received support from BCKDF, CANARIE, CRC and DRAC, Canada; CERN-CZ, FORTE and PRIMUS, Czech Republic; COST, ERC, ERDF, Horizon 2020, ICSC-NextGenerationEU and Marie Skłodowska-Curie Actions, European Union; Investissements d'Avenir Labex, Investissements d'Avenir Idex and ANR, France; DFG and AvH Foundation, Germany; Herakleitos, Thales and Aristeia programmes co-financed by EU-ESF and the Greek NSRF, Greece; BSF-NSF and MINERVA, Israel; NCN and NAWA, Poland; La Caixa Banking Foundation, CERCA Programme Generalitat de Catalunya and PROMETEO and GenT Programmes Generalitat Valenciana, Spain; Göran Gustafssons Stiftelse, Sweden; The Royal Society and Leverhulme Trust, United Kingdom.

In addition, individual members wish to acknowledge support from Armenia: Yerevan Physics Institute (FAPERJ); CERN: European Organization for Nuclear Research (CERN PJAS); Chile: Agencia Nacional de Investigación y Desarrollo (FONDECYT 1230812, FONDECYT 1230987, FONDECYT 1240864); China: Chinese Ministry of Science and Technology (MOST-2023YFA1605700, MOST-2023YFA1609300), National Natural Science Foundation of China (NSFC - 12175119, NSFC 12275265, NSFC-12075060); Czech Republic: Czech Science Foundation (GACR - 24-11373S), Ministry of Education Youth and Sports (ERC-CZ-LL2327, FORTE CZ.02.01.01/00/22_008/0004632), PRIMUS Research Programme (PRIMUS/21/SCI/017); EU: H2020 European Research Council (ERC - 101002463); European Union: European Research Council (ERC - 948254, ERC 101089007), Horizon 2020 Framework Programme (MUCCA - CHIST-ERA-19-XAI-00), European Union, Future Artificial Intelligence Research (FAIR-NextGenerationEU PE00000013), Italian Center for High Performance Computing, Big Data and Quantum Computing (ICSC, NextGenerationEU); France: Agence Nationale de la Recherche (ANR-20-CE31-0013, ANR-21-CE31-0013, ANR-21-CE31-0022, ANR-22-EDIR-0002), Investissements d'Avenir Labex (ANR-11-LABX-0012); Germany: Baden-Württemberg Stiftung (BW Stiftung-Postdoc

JHEP07(2025)086

Eliteprogramme), Deutsche Forschungsgemeinschaft (DFG - 469666862, DFG - CR 312/5-2); Italy: Istituto Nazionale di Fisica Nucleare (ICSC, NextGenerationEU), Ministero dell'Università e della Ricerca (NextGenEU PRIN20223N7F8K M4C2.1.1); Japan: Japan Society for the Promotion of Science (JSPS KAKENHI JP22H01227, JSPS KAKENHI JP22H04944, JSPS KAKENHI JP22KK0227, JSPS KAKENHI JP23KK0245); Netherlands: Netherlands Organisation for Scientific Research (NWO Veni 2020 - VI.Veni.202.179); Norway: Research Council of Norway (RCN-314472); Poland: Ministry of Science and Higher Education (IDUB AGH, POB8, D4 no 9722), Polish National Agency for Academic Exchange (PPN/PPO/2020/1/00002/U/00001), Polish National Science Centre (NCN 2021/42/E/ST2/00350, NCN OPUS nr 2022/47/B/ST2/03059, NCN UMO-2019/34/E/ST2/00393, NCN & H2020 MSCA 945339, UMO-2020/37/B/ST2/01043, UMO-2021/40/C/ST2/00187, UMO-2022/47/O/ST2/00148, UMO-2023/49/B/ST2/04085, UMO-2023/51/B/ST2/00920); Portugal: Foundation for Science and Technology (FCT); Slovenia: Slovenian Research Agency (ARIS grant J1-3010); Spain: Generalitat Valenciana (Artemisa, FEDER, IDIFEDER/2018/048), Ministry of Science and Innovation (MCIN & NextGenEU PCI2022-135018-2, MICIN & FEDER PID2021-125273NB, RYC2019-028510-I, RYC2020-030254-I, RYC2021-031273-I, RYC2022-038164-I), PROMETEO and GenT Programmes Generalitat Valenciana (CIDEGENT/2019/027); Sweden: Carl Trygger Foundation (Carl Trygger Foundation CTS 22:2312), Swedish Research Council (Swedish Research Council 2023-04654, VR 2018-00482, VR 2021-03651, VR 2022-03845, VR 2022-04683, VR 2023-03403), Knut and Alice Wallenberg Foundation (KAW 2018.0157, KAW 2018.0458, KAW 2019.0447, KAW 2022.0358); Switzerland: Swiss National Science Foundation (SNSF - PCEFP2_194658); United Kingdom: Leverhulme Trust (Leverhulme Trust RPG-2020-004), Royal Society (NIF-R1-231091); United States of America: U.S. Department of Energy (ECA DE-AC02-76SF00515), Neubauer Family Foundation.

Data Availability Statement. This article has no associated data or the data will not be deposited.

Code Availability Statement. This article has no associated code or the code will not be deposited.

References

[1] B.A. Kniehl, G. Kramer, I. Schienbein and H. Spiesberger, *Reconciling open charm production at the Fermilab Tevatron with QCD*, *Phys. Rev. Lett.* **96** (2006) 012001 [hep-ph/0508129] [INSPIRE].

[2] B.A. Kniehl, G. Kramer, I. Schienbein and H. Spiesberger, *Inclusive charmed-meson production at the CERN LHC*, *Eur. Phys. J. C* **72** (2012) 2082 [arXiv:1202.0439] [INSPIRE].

[3] Particle Data Group collaboration, *Review of particle physics*, *Phys. Rev. D* **110** (2024) 030001 [INSPIRE].

[4] ATLAS collaboration, *Prospects for lepton flavour violation measurements in $\tau \to 3\mu$ decays with the ATLAS detector at the HL-LHC*, ATL-PHYS-PUB-2018-032, CERN, Geneva, Switzerland (2018).

[5] L. Evans and P. Bryant, *LHC machine*, 2008 *JINST* **3** S08001 [INSPIRE].

[6] ALICE collaboration, *Charm production and fragmentation fractions at midrapidity in pp collisions at $\sqrt{s} = 13$ TeV*, *JHEP* **12** (2023) 086 [arXiv:2308.04877] [INSPIRE].

[7] ALICE collaboration, *Measurement of beauty-quark production in pp collisions at $\sqrt{s} = 13$ TeV via non-prompt D mesons*, *JHEP* **10** (2024) 110 [arXiv:2402.16417] [INSPIRE].

[8] ALICE collaboration, *Measurement of charm production at central rapidity in proton-proton collisions at $\sqrt{s} = 2.76$ TeV*, *JHEP* **07** (2012) 191 [arXiv:1205.4007] [INSPIRE].

[9] ALICE collaboration, *Measurement of* D^0 , D^+ , D^{*+} *and* D_s^+ *production in pp collisions at* $\sqrt{s} = 5.02$ *TeV with ALICE*, *Eur. Phys. J. C* **79** (2019) 388 [arXiv:1901.07979] [INSPIRE].

[10] ALICE collaboration, *Measurement of D-meson production at mid-rapidity in pp collisions at $\sqrt{s} = 7$ TeV*, *Eur. Phys. J. C* **77** (2017) 550 [arXiv:1702.00766] [INSPIRE].

[11] ALICE collaboration, *Measurement of beauty and charm production in pp collisions at $\sqrt{s} = 5.02$ TeV via non-prompt and prompt D mesons*, *JHEP* **05** (2021) 220 [arXiv:2102.13601] [INSPIRE].

[12] CMS collaboration, *Measurement of prompt open-charm production cross sections in proton-proton collisions at $\sqrt{s} = 13$ TeV*, *JHEP* **11** (2021) 225 [arXiv:2107.01476] [INSPIRE].

[13] LHCb collaboration, *Measurements of prompt charm production cross-sections in pp collisions at $\sqrt{s} = 13$ TeV*, *JHEP* **03** (2016) 159 [*Erratum ibid.* **09** (2016) 013] [arXiv:1510.01707] [INSPIRE].

[14] LHCb collaboration, *Measurements of prompt charm production cross-sections in pp collisions at $\sqrt{s} = 5$ TeV*, *JHEP* **06** (2017) 147 [arXiv:1610.02230] [INSPIRE].

[15] LHCb collaboration, *Prompt charm production in pp collisions at $\sqrt{s} = 7$ TeV*, *Nucl. Phys. B* **871** (2013) 1 [arXiv:1302.2864] [INSPIRE].

[16] ATLAS collaboration, *Measurement of $D^{*\pm}$, $D^\pm$ and $D_s^\pm$ meson production cross sections in pp collisions at $\sqrt{s} = 7$ TeV with the ATLAS detector*, *Nucl. Phys. B* **907** (2016) 717 [arXiv:1512.02913] [INSPIRE].

[17] ATLAS collaboration, *The ATLAS experiment at the CERN Large Hadron Collider*, 2008 *JINST* **3** S08003 [INSPIRE].

[18] ATLAS collaboration, *ATLAS Insertable B-Layer technical design report*, ATLAS-TDR-19, CERN, Geneva, Switzerland (2010).

[19] ATLAS IBL collaboration, *Production and integration of the ATLAS Insertable B-Layer*, 2018 *JINST* **13** T05008 [arXiv:1803.00844] [INSPIRE].

[20] G. Avoni et al., *The new LUCID-2 detector for luminosity measurement and monitoring in ATLAS*, 2018 *JINST* **13** P07017 [INSPIRE].

[21] ATLAS collaboration, *Performance of the ATLAS trigger system in 2015*, *Eur. Phys. J. C* **77** (2017) 317 [arXiv:1611.09661] [INSPIRE].

[22] ATLAS collaboration, *Software and computing for run 3 of the ATLAS experiment at the LHC*, *Eur. Phys. J. C* **85** (2025) 234 [arXiv:2404.06335] [INSPIRE].

[23] ATLAS collaboration, *ATLAS data quality operations and performance for 2015–2018 data-taking*, 2020 *JINST* **15** P04003 [arXiv:1911.04632] [INSPIRE].

[24] ATLAS collaboration, *Luminosity determination in pp collisions at* $\sqrt{s} = 13$ *TeV using the ATLAS detector at the LHC*, Eur. Phys. J. C **83** (2023) 982 [arXiv:2212.09379] [INSPIRE].

[25] T. Sjöstrand et al., *An introduction to PYTHIA 8.2*, Comput. Phys. Commun. **191** (2015) 159 [arXiv:1410.3012] [INSPIRE].

[26] R.D. Ball et al., *Parton distributions with LHC data*, Nucl. Phys. B **867** (2013) 244 [arXiv:1207.1303] [INSPIRE].

[27] ATLAS collaboration, *ATLAS Pythia 8 tunes to 7 TeV data*, ATL-PHYS-PUB-2014-021, CERN, Geneva, Switzerland (2014).

[28] ATLAS collaboration, *The ATLAS simulation infrastructure*, Eur. Phys. J. C **70** (2010) 823 [arXiv:1005.4568] [INSPIRE].

[29] GEANT4 collaboration, *GEANT4 — a simulation toolkit*, Nucl. Instrum. Meth. A **506** (2003) 250 [INSPIRE].

[30] T. Sjöstrand, S. Mrenna and P.Z. Skands, *A brief introduction to PYTHIA 8.1*, Comput. Phys. Commun. **178** (2008) 852 [arXiv:0710.3820] [INSPIRE].

[31] ATLAS collaboration, *The Pythia 8 A3 tune description of ATLAS minimum bias and inelastic measurements incorporating the Donnachie-Landshoff diffractive model*, ATL-PHYS-PUB-2016-017, CERN, Geneva, Switzerland (2016).

[32] B.A. Kniehl, G. Kramer, I. Schienbein and H. Spiesberger, *Inclusive* $D^{*\pm}$ *production in* $p\bar{p}$ *collisions with massive charm quarks*, Phys. Rev. D **71** (2005) 014018 [hep-ph/0410289] [INSPIRE].

[33] B.A. Kniehl, G. Kramer, I. Schienbein and H. Spiesberger, *Open charm hadroproduction and the charm content of the proton*, Phys. Rev. D **79** (2009) 094009 [arXiv:0901.4130] [INSPIRE].

[34] M. Benzke et al., *Prompt neutrinos from atmospheric charm in the general-mass variable-flavor-number scheme*, JHEP **12** (2017) 021 [arXiv:1705.10386] [INSPIRE].

[35] B.A. Kniehl and G. Kramer, D^0, D^+, D_s^+, *and* Λ_c^+ *fragmentation functions from CERN LEP1*, Phys. Rev. D **71** (2005) 094013 [hep-ph/0504058] [INSPIRE].

[36] M. Cacciari, M. Greco and P. Nason, *The* p_T *spectrum in heavy-flavour hadroproduction*, JHEP **05** (1998) 007 [hep-ph/9803400] [INSPIRE].

[37] M. Cacciari et al., *Theoretical predictions for charm and bottom production at the LHC*, JHEP **10** (2012) 137 [arXiv:1205.6344] [INSPIRE].

[38] S. Dulat et al., *New parton distribution functions from a global analysis of quantum chromodynamics*, Phys. Rev. D **93** (2016) 033006 [arXiv:1506.07443] [INSPIRE].

[39] T. Kneesch, B.A. Kniehl, G. Kramer and I. Schienbein, *Charmed-meson fragmentation functions with finite-mass corrections*, Nucl. Phys. B **799** (2008) 34 [arXiv:0712.0481] [INSPIRE].

[40] M. Cacciari, S. Frixione and P. Nason, *The* p_T *spectrum in heavy flavor photoproduction*, JHEP **03** (2001) 006 [hep-ph/0102134] [INSPIRE].

[41] M. Cacciari, M.L. Mangano and P. Nason, *Gluon PDF constraints from the ratio of forward heavy-quark production at the LHC at* $\sqrt{s} = 7$ *and* 13 *TeV*, Eur. Phys. J. C **75** (2015) 610 [arXiv:1507.06197] [INSPIRE].

[42] NNPDF collaboration, *Parton distributions for the LHC run II*, JHEP **04** (2015) 040 [arXiv:1410.8849] [INSPIRE].

[43] L. Gladilin, *Fragmentation fractions of c and b quarks into charmed hadrons at LEP*, *Eur. Phys. J. C* **75** (2015) 19 [arXiv:1404.3888] [INSPIRE].

[44] ATLAS collaboration, *Performance of the ATLAS muon triggers in run 2*, 2020 *JINST* **15** P09015 [arXiv:2004.13447] [INSPIRE].

[45] ATLAS collaboration, *Muon reconstruction and identification efficiency in ATLAS using the full run 2 pp collision data set at* $\sqrt{s} = 13$ *TeV*, *Eur. Phys. J. C* **81** (2021) 578 [arXiv:2012.00578] [INSPIRE].

[46] ATLAS collaboration, *Early inner detector tracking performance in the 2015 data at* $\sqrt{s} = 13$ *TeV*, ATL-PHYS-PUB-2015-051, CERN, Geneva, Switzerland (2015).

[47] ATLAS collaboration, *Vertex reconstruction performance of the ATLAS detector at* $\sqrt{s} = 13$ *TeV*, ATL-PHYS-PUB-2015-026, CERN, Geneva, Switzerland (2015).

[48] W. Voigt, *On the law of intensity distribution within the lines of a gas spectrum*, volume 1912,25 of *Meeting reports*, Munich, Germany (1912).

[49] W. Verkerke and D.P. Kirkby, *The RooFit toolkit for data modeling*, *eConf C* **0303241** (2003) MOLT007 [physics/0306116] [INSPIRE].

[50] ATLAS collaboration, *Studies of the muon momentum calibration and performance of the ATLAS detector with pp collisions at* $\sqrt{s} = 13$ *TeV*, *Eur. Phys. J. C* **83** (2023) 686 [arXiv:2212.07338] [INSPIRE].

[51] ATLAS collaboration, *Performance of the ATLAS track reconstruction algorithms in dense environments in LHC run 2*, *Eur. Phys. J. C* **77** (2017) 673 [arXiv:1704.07983] [INSPIRE].

[52] ATLAS collaboration, *Measurement of Upsilon production in 7 TeV pp collisions at ATLAS*, *Phys. Rev. D* **87** (2013) 052004 [arXiv:1211.7255] [INSPIRE].

[53] A.D. Bukin, *Fitting function for asymmetric peaks*, arXiv:0711.4449 [INSPIRE].

[54] ATLAS collaboration, *ATLAS computing acknowledgements*, ATL-SOFT-PUB-2025-001, CERN, Geneva, Switzerland (2025).

JHEP07(2025)086

The ATLAS collaboration

G. Aad[104], E. Aakvaag[17], B. Abbott[123], S. Abdelhameed[119a], K. Abeling[56], N.J. Abicht[50], S.H. Abidi[30], M. Aboelela[45], A. Aboulhorma[36e], H. Abramowicz[155], H. Abreu[154], Y. Abulaiti[120], B.S. Acharya[70a,70b,l], A. Ackermann[64a], C. Adam Bourdarios[4], L. Adamczyk[87a], S.V. Addepalli[27], M.J. Addison[103], J. Adelman[118], A. Adiguzel[22c], T. Adye[137], A.A. Affolder[139], Y. Afik[40], M.N. Agaras[13], J. Agarwala[74a,74b], A. Aggarwal[102], C. Agheorghiesei[28c], F. Ahmadov[39,aa], W.S. Ahmed[106], S. Ahuja[97], X. Ai[63e], G. Aielli[77a,77b], A. Aikot[166], M. Ait Tamlihat[36e], B. Aitbenchikh[36a], M. Akbiyik[102], T.P.A. Åkesson[100], A.V. Akimov[38], D. Akiyama[171], N.N. Akolkar[25], S. Aktas[22a], K. Al Khoury[42], G.L. Alberghi[24b], J. Albert[168], P. Albicocco[54], G.L. Albouy[61], S. Alderweireldt[53], Z.L. Alegria[124], M. Aleksa[37], I.N. Aleksandrov[39], C. Alexa[28b], T. Alexopoulos[10], F. Alfonsi[24b], M. Algren[57], M. Alhroob[170], B. Ali[135], H.M.J. Ali[93,t], S. Ali[32], S.W. Alibocus[94], M. Aliev[34c], G. Alimonti[72a], W. Alkakhi[56], C. Allaire[67], B.M.M. Allbrooke[150], J.S. Allen[103], J.F. Allen[53], C.A. Allendes Flores[140f], P.P. Allport[21], A. Aloisio[73a,73b], F. Alonso[92], C. Alpigiani[142], Z.M.K. Alsolami[93], M. Alvarez Estevez[101], A. Alvarez Fernandez[102], M. Alves Cardoso[57], M.G. Alviggi[73a,73b], M. Aly[103], Y. Amaral Coutinho[84b], A. Ambler[106], C. Amelung[37], M. Amerl[103], C.G. Ames[111], D. Amidei[108], B. Amini[55], K. Amirie[158], S.P. Amor Dos Santos[133a], K.R. Amos[166], D. Amperiadou[156], S. An[85], V. Ananiev[128], C. Anastopoulos[143], T. Andeen[11], J.K. Anders[37], A.C. Anderson[60], S.Y. Andrean[48a,48b], A. Andreazza[72a,72b], S. Angelidakis[9], A. Angerami[42], A.V. Anisenkov[38], A. Annovi[75a], C. Antel[57], E. Antipov[149], M. Antonelli[54], F. Anulli[76a], M. Aoki[85], T. Aoki[157], M.A. Aparo[150], L. Aperio Bella[49], C. Appelt[19], A. Apyan[27], S.J. Arbiol Val[88], C. Arcangeletti[54], A.T.H. Arce[52], J-F. Arguin[110], S. Argyropoulos[55], J.-H. Arling[49], O. Arnaez[4], H. Arnold[149], G. Artoni[76a,76b], H. Asada[113], K. Asai[121], S. Asai[157], N.A. Asbah[37], R.A. Ashby Pickering[170], K. Assamagan[30], R. Astalos[29a], K.S.V. Astrand[100], S. Atashi[162], R.J. Atkin[34a], M. Atkinson[165], H. Atmani[36f], P.A. Atmasiddha[131], K. Augsten[135], S. Auricchio[73a,73b], A.D. Auriol[21], V.A. Austrup[103], G. Avolio[37], K. Axiotis[57], G. Azuelos[110,af], D. Babal[29b], H. Bachacou[138], K. Bachas[156,p], A. Bachiu[35], F. Backman[48a,48b], A. Badea[40], T.M. Baer[108], P. Bagnaia[76a,76b], M. Bahmani[19], D. Bahner[55], K. Bai[126], J.T. Baines[137], L. Baines[96], O.K. Baker[175], E. Bakos[16], D. Bakshi Gupta[8], L.E. Balabram Filho[84b], V. Balakrishnan[123], R. Balasubramanian[4], E.M. Baldin[38], P. Balek[87a], E. Ballabene[24b,24a], F. Balli[138], L.M. Baltes[64a], W.K. Balunas[33], J. Balz[102], I. Bamwidhi[119b], E. Banas[88], M. Bandieramonte[132], A. Bandyopadhyay[25], S. Bansal[25], L. Barak[155], M. Barakat[49], E.L. Barberio[107], D. Barberis[58b,58a], M. Barbero[104], M.Z. Barel[117], T. Barillari[112], M-S. Barisits[37], T. Barklow[147], P. Baron[125], D.A. Baron Moreno[103], A. Baroncelli[63a], A.J. Barr[129], J.D. Barr[98], F. Barreiro[101], J. Barreiro Guimarães da Costa[14], U. Barron[155], M.G. Barros Teixeira[133a], S. Barsov[38], F. Bartels[64a], R. Bartoldus[147], A.E. Barton[93], P. Bartos[29a], A. Basan[102], M. Baselga[50], A. Bassalat[67,b], M.J. Basso[159a], S. Bataju[45], R. Bate[167], R.L. Bates[60], S. Batlamous[101], B. Batool[145], M. Battaglia[139], D. Battulga[19], M. Bauce[76a,76b], M. Bauer[80], P. Bauer[25], L.T. Bazzano Hurrell[31], J.B. Beacham[52], T. Beau[130], J.Y. Beaucamp[92], P.H. Beauchemin[161], P. Bechtle[25], H.P. Beck[20,o],

JHEP07(2025)086

K. Becker[170], A.J. Beddall[83], V.A. Bednyakov[39], C.P. Bee[149], L.J. Beemster[16], T.A. Beermann[37], M. Begalli[84d], M. Begel[30], A. Behera[149], J.K. Behr[49], J.F. Beirer[37], F. Beisiegel[25], M. Belfkir[119b], G. Bella[155], L. Bellagamba[24b], A. Bellerive[35], P. Bellos[21], K. Beloborodov[38], D. Benchekroun[36a], F. Bendebba[36a], Y. Benhammou[155], K.C. Benkendorfer[62], L. Beresford[49], M. Beretta[54], E. Bergeaas Kuutmann[164], N. Berger[4], B. Bergmann[135], J. Beringer[18a], G. Bernardi[5], C. Bernius[147], F.U. Bernlochner[25], F. Bernon[37], A. Berrocal Guardia[13], T. Berry[97], P. Berta[136], A. Berthold[51], S. Bethke[112], A. Betti[76a,76b], A.J. Bevan[96], N.K. Bhalla[55], S. Bhatta[149], D.S. Bhattacharya[169], P. Bhattarai[147], K.D. Bhide[55], V.S. Bhopatkar[124], R.M. Bianchi[132], G. Bianco[24b,24a], O. Biebel[111], R. Bielski[126], M. Biglietti[78a], C.S. Billingsley[45], Y. Bimgdi[36f], M. Bindi[56], A. Bingul[22b], C. Bini[76a,76b], G.A. Bird[33], M. Birman[172], M. Biros[136], S. Biryukov[150], T. Bisanz[50], E. Bisceglie[44b,44a], J.P. Biswal[137], D. Biswas[145], I. Bloch[49], A. Blue[60], U. Blumenschein[96], J. Blumenthal[102], V.S. Bobrovnikov[38], M. Boehler[55], B. Boehm[169], D. Bogavac[37], A.G. Bogdanchikov[38], L.S. Boggia[130], C. Bohm[48a], V. Boisvert[97], P. Bokan[37], T. Bold[87a], M. Bomben[5], M. Bona[96], M. Boonekamp[138], C.D. Booth[97], A.G. Borbély[60], I.S. Bordulev[38], G. Borissov[93], D. Bortoletto[129], D. Boscherini[24b], M. Bosman[13], J.D. Bossio Sola[37], K. Bouaouda[36a], N. Bouchhar[166], L. Boudet[4], J. Boudreau[132], E.V. Bouhova-Thacker[93], D. Boumediene[41], R. Bouquet[58b,58a], A. Boveia[122], J. Boyd[37], D. Boye[30], I.R. Boyko[39], L. Bozianu[57], J. Bracinik[21], N. Brahimi[4], G. Brandt[174], O. Brandt[33], F. Braren[49], B. Brau[105], J.E. Brau[126], R. Brener[172], L. Brenner[117], R. Brenner[164], S. Bressler[172], G. Brianti[79a,79b], D. Britton[60], D. Britzger[112], I. Brock[25], R. Brock[109], G. Brooijmans[42], E.M. Brooks[159b], E. Brost[30], L.M. Brown[168,159a], L.E. Bruce[62], T.L. Bruckler[129], P.A. Bruckman de Renstrom[88], B. Brüers[49], A. Bruni[24b], G. Bruni[24b], M. Bruschi[24b], N. Bruscino[76a,76b], T. Buanes[17], Q. Buat[142], D. Buchin[112], A.G. Buckley[60], O. Bulekov[38], B.A. Bullard[147], S. Burdin[94], C.D. Burgard[50], A.M. Burger[37], B. Burghgrave[8], O. Burlayenko[55], J. Burleson[165], J.T.P. Burr[33], J.C. Burzynski[146], E.L. Busch[42], V. Büscher[102], P.J. Bussey[60], J.M. Butler[26], C.M. Buttar[60], J.M. Butterworth[98], W. Buttinger[137], C.J. Buxo Vazquez[109], A.R. Buzykaev[38], S. Cabrera Urbán[166], L. Cadamuro[67], D. Caforio[59], H. Cai[132], Y. Cai[14,114c], Y. Cai[114a], V.M.M. Cairo[37], O. Cakir[3a], N. Calace[37], P. Calafiura[18a], G. Calderini[130], P. Calfayan[69], G. Callea[60], L.P. Caloba[84b], D. Calvet[41], S. Calvet[41], M. Calvetti[75a,75b], R. Camacho Toro[130], S. Camarda[37], D. Camarero Munoz[27], P. Camarri[77a,77b], M.T. Camerlingo[73a,73b], D. Cameron[37], C. Camincher[168], M. Campanelli[98], A. Camplani[43], V. Canale[73a,73b], A.C. Canbay[3a], E. Canonero[97], J. Cantero[166], Y. Cao[165], F. Capocasa[27], M. Capua[44b,44a], A. Carbone[72a,72b], R. Cardarelli[77a], J.C.J. Cardenas[8], G. Carducci[44b,44a], T. Carli[37], G. Carlino[73a], J.I. Carlotto[13], B.T. Carlson[132,q], E.M. Carlson[168,159a], J. Carmignani[94], L. Carminati[72a,72b], A. Carnelli[138], M. Carnesale[37], S. Caron[116], E. Carquin[140f], I.B. Carr[107], S. Carrá[72a], G. Carratta[24b,24a], A.M. Carroll[126], M.P. Casado[13,i], M. Caspar[49], F.L. Castillo[4], L. Castillo Garcia[13], V. Castillo Gimenez[166], N.F. Castro[133a,133e], A. Catinaccio[37], J.R. Catmore[128], T. Cavaliere[4], V. Cavaliere[30], N. Cavalli[24b,24a], L.J. Caviedes Betancourt[23b], Y.C. Cekmecelioglu[49], E. Celebi[83], S. Cella[37], M.S. Centonze[71a,71b], V. Cepaitis[57], K. Cerny[125], A.S. Cerqueira[84a], A. Cerri[150], L. Cerrito[77a,77b], F. Cerutti[18a], B. Cervato[145], A. Cervelli[24b], G. Cesarini[54], S.A. Cetin[83], D. Chakraborty[118], J. Chan[18a], W.Y. Chan[157], J.D. Chapman[33], E. Chapon[138], B. Chargeishvili[153b], D.G. Charlton[21], M. Chatterjee[20], C. Chauhan[136], Y. Che[114a], S. Chekanov[6], S.V. Chekulaev[159a], G.A. Chelkov[39,a], A. Chen[108], B. Chen[155], B. Chen[168], H. Chen[114a], H. Chen[30], J. Chen[63c], J. Chen[146], M. Chen[129], S. Chen[89], S.J. Chen[114a], X. Chen[63c], X. Chen[15,ae], Y. Chen[63a], C.L. Cheng[173], H.C. Cheng[65a], S. Cheong[147], A. Cheplakov[39], E. Cheremushkina[49], E. Cherepanova[117], R. Cherkaoui El Moursli[36e], E. Cheu[7], K. Cheung[66], L. Chevalier[138], V. Chiarella[54], G. Chiarelli[75a], N. Chiedde[104], G. Chiodini[71a], A.S. Chisholm[21], A. Chitan[28b], M. Chitishvili[166], M.V. Chizhov[39,r], K. Choi[11], Y. Chou[142], E.Y.S. Chow[116], K.L. Chu[172], M.C. Chu[65a], X. Chu[14,114c], Z. Chubinidze[54], J. Chudoba[134], J.J. Chwastowski[88], D. Cieri[112], K.M. Ciesla[87a], V. Cindro[95], A. Ciocio[18a], F. Cirotto[73a,73b], Z.H. Citron[172], M. Citterio[72a], D.A. Ciubotaru[28b], A. Clark[57], P.J. Clark[53], N. Clarke Hall[98], C. Clarry[158], J.M. Clavijo Columbie[49], S.E. Clawson[49], C. Clement[48a,48b], Y. Coadou[104], M. Cobal[70a,70c], A. Coccaro[58b], R.F. Coelho Barrue[133a], R. Coelho Lopes De Sa[105], S. Coelli[72a], B. Cole[42], J. Collot[61], P. Conde Muiño[133a,133g], M.P. Connell[34c], S.H. Connell[34c], E.I. Conroy[129], F. Conventi[73a,ag], H.G. Cooke[21], A.M. Cooper-Sarkar[129], F.A. Corchia[24b,24a], A. Cordeiro Oudot Choi[130], L.D. Corpe[41], M. Corradi[76a,76b], F. Corriveau[106,y], A. Cortes-Gonzalez[19], M.J. Costa[166], F. Costanza[4], D. Costanzo[143], B.M. Cote[122], J. Couthures[4], G. Cowan[97], K. Cranmer[173], L. Cremer[50], D. Cremonini[24b,24a], S. Crépé-Renaudin[61], F. Crescioli[130], M. Cristinziani[145], M. Cristoforetti[79a,79b], V. Croft[117], J.E. Crosby[124], G. Crosetti[44b,44a], A. Cueto[101], H. Cui[98], Z. Cui[7], W.R. Cunningham[60], F. Curcio[166], J.R. Curran[53], P. Czodrowski[37], M.J. Da Cunha Sargedas De Sousa[58b,58a], J.V. Da Fonseca Pinto[84b], C. Da Via[103], W. Dabrowski[87a], T. Dado[37], S. Dahbi[152], T. Dai[108], D. Dal Santo[20], C. Dallapiccola[105], M. Dam[43], G. D'amen[30], V. D'Amico[111], J. Damp[102], J.R. Dandoy[35], D. Dannheim[37], M. Danninger[146], V. Dao[149], G. Darbo[58b], S.J. Das[30], F. Dattola[49], S. D'Auria[72a,72b], A. D'Avanzo[73a,73b], C. David[34a], T. Davidek[136], I. Dawson[96], H.A. Day-hall[135], K. De[8], R. De Asmundis[73a], N. De Biase[49], S. De Castro[24b,24a], N. De Groot[116], P. de Jong[117], H. De la Torre[118], A. De Maria[114a], A. De Salvo[76a], U. De Sanctis[77a,77b], F. De Santis[71a,71b], A. De Santo[150], J.B. De Vivie De Regie[61], J. Debevc[95], D.V. Dedovich[39], J. Degens[94], A.M. Deiana[45], F. Del Corso[24b,24a], J. Del Peso[101], L. Delagrange[130], F. Deliot[138], C.M. Delitzsch[50], M. Della Pietra[73a,73b], D. Della Volpe[57], A. Dell'Acqua[37], L. Dell'Asta[72a,72b], M. Delmastro[4], P.A. Delsart[61], S. Demers[175], M. Demichev[39], S.P. Denisov[38], L. D'Eramo[41], D. Derendarz[88], F. Derue[130], P. Dervan[94], K. Desch[25], C. Deutsch[25], F.A. Di Bello[58b,58a], A. Di Ciaccio[77a,77b], L. Di Ciaccio[4], A. Di Domenico[76a,76b], C. Di Donato[73a,73b], A. Di Girolamo[37], G. Di Gregorio[37], A. Di Luca[79a,79b], B. Di Micco[78a,78b], R. Di Nardo[78a,78b], K.F. Di Petrillo[40], M. Diamantopoulou[35], F.A. Dias[117], T. Dias Do Vale[146], M.A. Diaz[140a,140b], F.G. Diaz Capriles[25], A.R. Didenko[39], M. Didenko[166], E.B. Diehl[108], S. Díez Cornell[49], C. Diez Pardos[145], C. Dimitriadi[164], A. Dimitrievska[21], J. Dingfelder[25], T. Dingley[129], I-M. Dinu[28b], S.J. Dittmeier[64b], F. Dittus[37], M. Divisek[136], B. Dixit[94], F. Djama[104],

T. Djobava[153b], C. Doglioni[103,100], A. Dohnalova[29a], J. Dolejsi[136], Z. Dolezal[136], K. Domijan[87a], K.M. Dona[40], M. Donadelli[84d], B. Dong[109], J. Donini[41], A. D'Onofrio[73a,73b], M. D'Onofrio[94], J. Dopke[137], A. Doria[73a], N. Dos Santos Fernandes[133a], P. Dougan[103], M.T. Dova[92], A.T. Doyle[60], M.A. Draguet[129], M.P. Drescher[56], E. Dreyer[172], I. Drivas-koulouris[10], M. Drnevich[120], M. Drozdova[57], D. Du[63a], T.A. du Pree[117], F. Dubinin[38], M. Dubovsky[29a], E. Duchovni[172], G. Duckeck[111], O.A. Ducu[28b], D. Duda[53], A. Dudarev[37], E.R. Duden[27], M. D'uffizi[103], L. Duflot[67], M. Dührssen[37], I. Duminica[28g], A.E. Dumitriu[28b], M. Dunford[64a], S. Dungs[50], K. Dunne[48a,48b], A. Duperrin[104], H. Duran Yildiz[3a], M. Düren[59], A. Durglishvili[153b], D. Duvnjak[35], B.L. Dwyer[118], G.I. Dyckes[18a], M. Dyndal[87a], B.S. Dziedzic[37], Z.O. Earnshaw[150], G.H. Eberwein[129], B. Eckerova[29a], S. Eggebrecht[56], E. Egidio Purcino De Souza[84e], L.F. Ehrke[57], G. Eigen[17], K. Einsweiler[18a], T. Ekelof[164], P.A. Ekman[100], S. El Farkh[36b], Y. El Ghazali[63a], H. El Jarrari[37], A. El Moussaouy[36a], V. Ellajosyula[164], M. Ellert[164], F. Ellinghaus[174], N. Ellis[37], J. Elmsheuser[30], M. Elsawy[119a], M. Elsing[37], D. Emeliyanov[137], Y. Enari[85], I. Ene[18a], S. Epari[13], P.A. Erland[88], D. Ernani Martins Neto[88], M. Errenst[174], M. Escalier[67], C. Escobar[166], E. Etzion[155], G. Evans[133a,133b], H. Evans[69], L.S. Evans[97], A. Ezhilov[38], S. Ezzarqtouni[36a], F. Fabbri[24b,24a], L. Fabbri[24b,24a], G. Facini[98], V. Fadeyev[139], R.M. Fakhrutdinov[38], D. Fakoudis[102], S. Falciano[76a], L.F. Falda Ulhoa Coelho[37], F. Fallavollita[112], G. Falsetti[44b,44a], J. Faltova[136], C. Fan[165], K.Y. Fan[65b], Y. Fan[14], Y. Fang[14,114c], M. Fanti[72a,72b], M. Faraj[70a,70b], Z. Farazpay[99], A. Farbin[8], A. Farilla[78a], T. Farooque[109], S.M. Farrington[53], F. Fassi[36e], D. Fassouliotis[9], M. Faucci Giannelli[77a,77b], W.J. Fawcett[33], L. Fayard[67], P. Federic[136], P. Federicova[134], O.L. Fedin[38,a], M. Feickert[173], L. Feligioni[104], D.E. Fellers[126], C. Feng[63b], Z. Feng[117], M.J. Fenton[162], L. Ferencz[49], R.A.M. Ferguson[93], S.I. Fernandez Luengo[140f], P. Fernandez Martinez[68], M.J.V. Fernoux[104], J. Ferrando[93], A. Ferrari[164], P. Ferrari[117,116], R. Ferrari[74a], D. Ferrere[57], C. Ferretti[108], D. Fiacco[76a,76b], F. Fiedler[102], P. Fiedler[135], S. Filimonov[38], A. Filipčič[95], E.K. Filmer[1], F. Filthaut[116], M.C.N. Fiolhais[133a,133c,c], L. Fiorini[166], W.C. Fisher[109], T. Fitschen[103], P.M. Fitzhugh[138], I. Fleck[145], P. Fleischmann[108], T. Flick[174], M. Flores[34d,ac], L.R. Flores Castillo[65a], L. Flores Sanz De Acedo[37], F.M. Follega[79a,79b], N. Fomin[33], J.H. Foo[158], A. Formica[138], A.C. Forti[103], E. Fortin[37], A.W. Fortman[18a], M.G. Foti[18a], L. Fountas[9,j], D. Fournier[67], H. Fox[93], P. Francavilla[75a,75b], S. Francescato[62], S. Franchellucci[57], M. Franchini[24b,24a], S. Franchino[64a], D. Francis[37], L. Franco[116], V. Franco Lima[37], L. Franconi[49], M. Franklin[62], G. Frattari[27], Y.Y. Frid[155], J. Friend[60], N. Fritzsche[37], A. Froch[55], D. Froidevaux[37], J.A. Frost[129], Y. Fu[63a], S. Fuenzalida Garrido[140f], M. Fujimoto[104], K.Y. Fung[65a], E. Furtado De Simas Filho[84e], M. Furukawa[157], J. Fuster[166], A. Gaa[56], A. Gabrielli[24b,24a], A. Gabrielli[158], P. Gadow[37], G. Gagliardi[58b,58a], L.G. Gagnon[18a], S. Gaid[163], S. Galantzan[155], J. Gallagher[1], E.J. Gallas[129], B.J. Gallop[137], K.K. Gan[122], S. Ganguly[157], Y. Gao[53], F.M. Garay Walls[140a,140b], B. Garcia[30], C. García[166], A. Garcia Alonso[117], A.G. Garcia Caffaro[175], J.E. García Navarro[166], M. Garcia-Sciveres[18a], G.L. Gardner[131], R.W. Gardner[40], N. Garelli[161], D. Garg[81], R.B. Garg[147], J.M. Gargan[53], C.A. Garner[158], C.M. Garvey[34a], V.K. Gassmann[161], G. Gaudio[74a],

V. Gautam[13], P. Gauzzi[76a,76b], J. Gavranovic[95], I.L. Gavrilenko[38], A. Gavrilyuk[38], C. Gay[167], G. Gaycken[126], E.N. Gazis[10], A.A. Geanta[28b], C.M. Gee[139], A. Gekow[122], C. Gemme[58b], M.H. Genest[61], A.D. Gentry[115], S. George[97], W.F. George[21], T. Geralis[47], P. Gessinger-Befurt[37], M.E. Geyik[174], M. Ghani[170], K. Ghorbanian[96], A. Ghosal[145], A. Ghosh[162], A. Ghosh[7], B. Giacobbe[24b], S. Giagu[76a,76b], T. Giani[117], A. Giannini[63a], S.M. Gibson[97], M. Gignac[139], D.T. Gil[87b], A.K. Gilbert[87a], B.J. Gilbert[42], D. Gillberg[35], G. Gilles[117], L. Ginabat[130], D.M. Gingrich[2,af], M.P. Giordani[70a,70c], P.F. Giraud[138], G. Giugliarelli[70a,70c], D. Giugni[72a], F. Giuli[77a,77b], I. Gkialas[9,j], L.K. Gladilin[38], C. Glasman[101], G.R. Gledhill[126], G. Glemža[49], M. Glisic[126], I. Gnesi[44b], Y. Go[30], M. Goblirsch-Kolb[37], B. Gocke[50], D. Godin[110], B. Gokturk[22a], S. Goldfarb[107], T. Golling[57], M.G.D. Gololo[34g], D. Golubkov[38], J.P. Gombas[109], A. Gomes[133a,133b], G. Gomes Da Silva[145], A.J. Gomez Delegido[166], R. Gonçalo[133a], L. Gonella[21], A. Gongadze[153c], F. Gonnella[21], J.L. Gonski[147], R.Y. González Andana[53], S. González de la Hoz[166], R. Gonzalez Lopez[94], C. Gonzalez Renteria[18a], M.V. Gonzalez Rodrigues[49], R. Gonzalez Suarez[164], S. Gonzalez-Sevilla[57], L. Goossens[37], B. Gorini[37], E. Gorini[71a,71b], A. Gorišek[95], T.C. Gosart[131], A.T. Goshaw[52], M.I. Gostkin[39], S. Goswami[124], C.A. Gottardo[37], S.A. Gotz[111], M. Gouighri[36b], V. Goumarre[49], A.G. Goussiou[142], N. Govender[34c], R.P. Grabarczyk[129], I. Grabowska-Bold[87a], K. Graham[35], E. Gramstad[128], S. Grancagnolo[71a,71b], C.M. Grant[1,138], P.M. Gravila[28f], F.G. Gravili[71a,71b], H.M. Gray[18a], M. Greco[71a,71b], M.J. Green[1], C. Grefe[25], A.S. Grefsrud[17], I.M. Gregor[49], K.T. Greif[162], P. Grenier[147], S.G. Grewe[112], A.A. Grillo[139], K. Grimm[32], S. Grinstein[13,u], J.-F. Grivaz[67], E. Gross[172], J. Grosse-Knetter[56], L. Guan[108], J.G.R. Guerrero Rojas[166], G. Guerrieri[37], R. Gugel[102], J.A.M. Guhit[108], A. Guida[19], E. Guilloton[170], S. Guindon[37], F. Guo[14,114c], J. Guo[63c], L. Guo[49], Y. Guo[108], A. Gupta[50], R. Gupta[132], S. Gurbuz[25], S.S. Gurdasani[55], G. Gustavino[76a,76b], P. Gutierrez[123], L.F. Gutierrez Zagazeta[131], M. Gutsche[51], C. Gutschow[98], C. Gwenlan[129], C.B. Gwilliam[94], E.S. Haaland[128], A. Haas[120], M. Habedank[60], C. Haber[18a], H.K. Hadavand[8], A. Hadef[51], S. Hadzic[112], A.I. Hagan[93], J.J. Hahn[145], E.H. Haines[98], M. Haleem[169], J. Haley[124], G.D. Hallewell[104], L. Halser[20], K. Hamano[168], M. Hamer[25], E.J. Hampshire[97], J. Han[63b], L. Han[114a], L. Han[63a], S. Han[18a], Y.F. Han[158], K. Hanagaki[85], M. Hance[139], D.A. Hangal[42], H. Hanif[146], M.D. Hank[131], J.B. Hansen[43], P.H. Hansen[43], D. Harada[57], T. Harenberg[174], S. Harkusha[38], M.L. Harris[105], Y.T. Harris[25], J. Harrison[13], N.M. Harrison[122], P.F. Harrison[170], N.M. Hartman[112], N.M. Hartmann[111], R.Z. Hasan[97,137], Y. Hasegawa[144], F. Haslbeck[129], S. Hassan[17], R. Hauser[109], C.M. Hawkes[21], R.J. Hawkings[37], Y. Hayashi[157], D. Hayden[109], C. Hayes[108], R.L. Hayes[117], C.P. Hays[129], J.M. Hays[96], H.S. Hayward[94], F. He[63a], M. He[14,114c], Y. He[49], Y. He[98], N.B. Heatley[96], V. Hedberg[100], A.L. Heggelund[128], N.D. Hehir[96,*], C. Heidegger[55], K.K. Heidegger[55], J. Heilman[35], S. Heim[49], T. Heim[18a], J.G. Heinlein[131], J.J. Heinrich[126], L. Heinrich[112,ad], J. Hejbal[134], A. Held[173], S. Hellesund[17], C.M. Helling[167], S. Hellman[48a,48b], R.C.W. Henderson[93], L. Henkelmann[33], A.M. Henriques Correia[37], H. Herde[100], Y. Hernández Jiménez[149], L.M. Herrmann[25], T. Herrmann[51], G. Herten[55], R. Hertenberger[111], L. Hervas[37], M.E. Hesping[102], N.P. Hessey[159a], J. Hessler[112],

M. Hidaoui[36b], N. Hidic[136], E. Hill[158], S.J. Hillier[21], J.R. Hinds[109], F. Hinterkeuser[25], M. Hirose[127], S. Hirose[160], D. Hirschbuehl[174], T.G. Hitchings[103], B. Hiti[95], J. Hobbs[149], R. Hobincu[28e], N. Hod[172], M.C. Hodgkinson[143], B.H. Hodkinson[129], A. Hoecker[37], D.D. Hofer[108], J. Hofer[166], T. Holm[25], M. Holzbock[37], L.B.A.H. Hommels[33], B.P. Honan[103], J.J. Hong[69], J. Hong[63c], T.M. Hong[132], B.H. Hooberman[165], W.H. Hopkins[6], M.C. Hoppesch[165], Y. Horii[113], M.E. Horstmann[112], S. Hou[152], A.S. Howard[95], J. Howarth[60], J. Hoya[6], M. Hrabovsky[125], A. Hrynevich[49], T. Hryn'ova[4], P.J. Hsu[66], S.-C. Hsu[142], T. Hsu[67], M. Hu[18a], Q. Hu[63a], S. Huang[65b], X. Huang[14,114c], Y. Huang[143], Y. Huang[102], Y. Huang[14], Z. Huang[103], Z. Hubacek[135], M. Huebner[25], F. Huegging[25], T.B. Huffman[129], M. Hufnagel Maranha De Faria[84a], C.A. Hugli[49], M. Huhtinen[37], S.K. Huiberts[17], R. Hulsken[106], N. Huseynov[12,g], J. Huston[109], J. Huth[62], R. Hyneman[147], G. Iacobucci[57], G. Iakovidis[30], L. Iconomidou-Fayard[67], J.P. Iddon[37], P. Iengo[73a,73b], R. Iguchi[157], Y. Iiyama[157], T. Iizawa[129], Y. Ikegami[85], N. Ilic[158], H. Imam[84c], G. Inacio Goncalves[84d], T. Ingebretsen Carlson[48a,48b], J.M. Inglis[96], G. Introzzi[74a,74b], M. Iodice[78a], V. Ippolito[76a,76b], R.K. Irwin[94], M. Ishino[157], W. Islam[173], C. Issever[19], S. Istin[22a,aj], H. Ito[171], R. Iuppa[79a,79b], A. Ivina[172], J.M. Izen[46], V. Izzo[73a], P. Jacka[134], P. Jackson[1], C.S. Jagfeld[111], G. Jain[159a], P. Jain[49], K. Jakobs[55], T. Jakoubek[172], J. Jamieson[60], W. Jang[157], M. Javurkova[105], P. Jawahar[103], L. Jeanty[126], J. Jejelava[153a,ab], P. Jenni[55,f], C.E. Jessiman[35], C. Jia[63b], H. Jia[167], J. Jia[149], X. Jia[14,114c], Z. Jia[114a], C. Jiang[53], S. Jiggins[49], J. Jimenez Pena[13], S. Jin[114a], A. Jinaru[28b], O. Jinnouchi[141], P. Johansson[143], K.A. Johns[7], J.W. Johnson[139], F.A. Jolly[49], D.M. Jones[150], E. Jones[49], K.S. Jones[8], P. Jones[33], R.W.L. Jones[93], T.J. Jones[94], H.L. Joos[56,37], R. Joshi[122], J. Jovicevic[16], X. Ju[18a], J.J. Junggeburth[105], T. Junkermann[64a], A. Juste Rozas[13,u], M.K. Juzek[88], S. Kabana[140e], A. Kaczmarska[88], M. Kado[112], H. Kagan[122], M. Kagan[147], A. Kahn[131], C. Kahra[102], T. Kaji[157], E. Kajomovitz[154], N. Kakati[172], I. Kalaitzidou[55], C.W. Kalderon[30], N.J. Kang[139], D. Kar[34g], K. Karava[129], M.J. Kareem[159b], E. Karentzos[55], O. Karkout[117], S.N. Karpov[39], Z.M. Karpova[39], V. Kartvelishvili[93], A.N. Karyukhin[38], E. Kasimi[156], J. Katzy[49], S. Kaur[35], K. Kawade[144], M.P. Kawale[123], C. Kawamoto[89], T. Kawamoto[63a], E.F. Kay[37], F.I. Kaya[161], S. Kazakos[109], V.F. Kazanin[38], Y. Ke[149], J.M. Keaveney[34a], R. Keeler[168], G.V. Kehris[62], J.S. Keller[35], J.J. Kempster[150], O. Kepka[134], B.P. Kerridge[137], S. Kersten[174], B.P. Kerševan[95], L. Keszeghova[29a], S. Ketabchi Haghighat[158], R.A. Khan[132], A. Khanov[124], A.G. Kharlamov[38], T. Kharlamova[38], E.E. Khoda[142], M. Kholodenko[133a], T.J. Khoo[19], G. Khoriauli[169], J. Khubua[153b,*], Y.A.R. Khwaira[130], B. Kibirige[34g], D. Kim[6], D.W. Kim[48a,48b], Y.K. Kim[40], N. Kimura[98], M.K. Kingston[56], A. Kirchhoff[56], C. Kirfel[25], F. Kirfel[25], J. Kirk[137], A.E. Kiryunin[112], S. Kita[160], C. Kitsaki[10], O. Kivernyk[25], M. Klassen[161], C. Klein[35], L. Klein[169], M.H. Klein[45], S.B. Klein[57], U. Klein[94], A. Klimentov[30], T. Klioutchnikova[37], P. Kluit[117], S. Kluth[112], E. Kneringer[80], T.M. Knight[158], A. Knue[50], M. Kobel[51], D. Kobylianskii[172], S.F. Koch[129], M. Kocian[147], P. Kodyš[136], D.M. Koeck[126], P.T. Koenig[25], T. Koffas[35], O. Kolay[51], I. Koletsou[4], T. Komarek[88], K. Köneke[55], A.X.Y. Kong[1], T. Kono[121], N. Konstantinidis[98], P. Kontaxakis[57], B. Konya[100], R. Kopeliansky[42], S. Koperny[87a],

K. Korcyl[88], K. Kordas[156,e], A. Korn[98], S. Korn[56], I. Korolkov[13], N. Korotkova[38], B. Kortman[117], O. Kortner[112], S. Kortner[112], W.H. Kostecka[118], V.V. Kostyukhin[145], A. Kotsokechagia[37], A. Kotwal[52], A. Koulouris[37], A. Kourkoumeli-Charalampidi[74a,74b], C. Kourkoumelis[9], E. Kourlitis[112], O. Kovanda[126], R. Kowalewski[168], W. Kozanecki[126], A.S. Kozhin[38], V.A. Kramarenko[38], G. Kramberger[95], P. Kramer[102], M.W. Krasny[130], A. Krasznahorkay[37], A.C. Kraus[118], J.W. Kraus[174], J.A. Kremer[49], T. Kresse[51], L. Kretschmann[174], J. Kretzschmar[94], K. Kreul[19], P. Krieger[158], M. Krivos[136], K. Krizka[21], K. Kroeninger[50], H. Kroha[112], J. Kroll[134], J. Kroll[131], K.S. Krowpman[109], U. Kruchonak[39], H. Krüger[25], N. Krumnack[82], M.C. Kruse[52], O. Kuchinskaia[38], S. Kuday[3a], S. Kuehn[37], R. Kuesters[55], T. Kuhl[49], V. Kukhtin[39], Y. Kulchitsky[38,a], S. Kuleshov[140d,140b], M. Kumar[34g], N. Kumari[49], P. Kumari[159b], A. Kupco[134], T. Kupfer[50], A. Kupich[38], O. Kuprash[55], H. Kurashige[86], L.L. Kurchaninov[159a], O. Kurdysh[67], Y.A. Kurochkin[38], A. Kurova[38], M. Kuze[141], A.K. Kvam[105], J. Kvita[125], T. Kwan[106], N.G. Kyriacou[108], L.A.O. Laatu[104], C. Lacasta[166], F. Lacava[76a,76b], H. Lacker[19], D. Lacour[130], N.N. Lad[98], E. Ladygin[39], A. Lafarge[41], B. Laforge[130], T. Lagouri[175], F.Z. Lahbabi[36a], S. Lai[56], J.E. Lambert[168], S. Lammers[69], W. Lampl[7], C. Lampoudis[156,e], G. Lamprinoudis[102], A.N. Lancaster[118], E. Lançon[30], U. Landgraf[55], M.P.J. Landon[96], V.S. Lang[55], O.K.B. Langrekken[128], A.J. Lankford[162], F. Lanni[37], K. Lantzsch[25], A. Lanza[74a], M. Lanzac Berrocal[166], J.F. Laporte[138], T. Lari[72a], F. Lasagni Manghi[24b], M. Lassnig[37], V. Latonova[134], A. Laurier[154], S.D. Lawlor[143], Z. Lawrence[103], R. Lazaridou[170], M. Lazzaroni[72a,72b], B. Le[103], H.D.M. Le[109], E.M. Le Boulicaut[175], L.T. Le Pottier[18a], B. Leban[24b,24a], A. Lebedev[82], M. LeBlanc[103], F. Ledroit-Guillon[61], S.C. Lee[152], S. Lee[48a,48b], T.F. Lee[94], L.L. Leeuw[34c], H.P. Lefebvre[97], M. Lefebvre[168], C. Leggett[18a], G. Lehmann Miotto[37], M. Leigh[57], W.A. Leight[105], W. Leinonen[116], A. Leisos[156,s], M.A.L. Leite[84c], C.E. Leitgeb[19], R. Leitner[136], K.J.C. Leney[45], T. Lenz[25], S. Leone[75a], C. Leonidopoulos[53], A. Leopold[148], R. Les[109], C.G. Lester[33], M. Levchenko[38], J. Levêque[4], L.J. Levinson[172], G. Levrini[24b,24a], M.P. Lewicki[88], C. Lewis[142], D.J. Lewis[4], L. Lewitt[143], A. Li[30], B. Li[63b], C. Li[63a], C-Q. Li[112], H. Li[63a], H. Li[63b], H. Li[114a], H. Li[15], H. Li[63b], J. Li[63c], K. Li[14], L. Li[63c], M. Li[14,114c], S. Li[14,114c], S. Li[63d,63c,d], T. Li[5], X. Li[106], Z. Li[157], Z. Li[14,114c], Z. Li[63a], S. Liang[14,114c], Z. Liang[14], M. Liberatore[138], B. Liberti[77a], K. Lie[65c], J. Lieber Marin[84e], H. Lien[69], H. Lin[108], K. Lin[109], R.E. Lindley[7], J.H. Lindon[2], J. Ling[62], E. Lipeles[131], A. Lipniacka[17], A. Lister[167], J.D. Little[69], B. Liu[14], B.X. Liu[114b], D. Liu[63d,63c], E.H.L. Liu[21], J.B. Liu[63a], J.K.K. Liu[33], K. Liu[63d], K. Liu[63d,63c], M. Liu[63a], M.Y. Liu[63a], P. Liu[14], Q. Liu[63d,142,63c], X. Liu[63a], X. Liu[63b], Y. Liu[114b,114c], Y.L. Liu[63b], Y.W. Liu[63a], S.L. Lloyd[96], E.M. Lobodzinska[49], P. Loch[7], E. Lodhi[158], T. Lohse[19], K. Lohwasser[143], E. Loiacono[49], M. Lokajicek[134,*], J.D. Lomas[21], J.D. Long[42], I. Longarini[162], R. Longo[165], I. Lopez Paz[68], A. Lopez Solis[49], N.A. Lopez-canelas[7], N. Lorenzo Martinez[4], A.M. Lory[111], M. Losada[119a], G. Löschcke Centeno[150], O. Loseva[38], X. Lou[48a,48b], X. Lou[14,114c], A. Lounis[67], P.A. Love[93], G. Lu[14,114c], M. Lu[67], S. Lu[131], Y.J. Lu[66], H.J. Lubatti[142], C. Luci[76a,76b], F.L. Lucio Alves[114a], F. Luehring[69], O. Lukianchuk[67], B.S. Lunday[131], O. Lundberg[148], B. Lund-Jensen[148,*], N.A. Luongo[6], M.S. Lutz[37],

JHEP07(2025)086

A.B. Lux[26], D. Lynn[30], R. Lysak[134], E. Lytken[100], V. Lyubushkin[39], T. Lyubushkina[39], M.M. Lyukova[149], M.Firdaus M. Soberi[53], H. Ma[30], K. Ma[63a], L.L. Ma[63b], W. Ma[63a], Y. Ma[124], J.C. MacDonald[102], P.C. Machado De Abreu Farias[84e], R. Madar[41], T. Madula[98], J. Maeda[86], T. Maeno[30], H. Maguire[143], V. Maiboroda[138], A. Maio[133a,133b,133d], K. Maj[87a], O. Majersky[49], S. Majewski[126], N. Makovec[67], V. Maksimovic[16], B. Malaescu[130], Pa. Malecki[88], V.P. Maleev[38], F. Malek[61,n], M. Mali[95], D. Malito[97], U. Mallik[81,*], S. Maltezos[10], S. Malyukov[39], J. Mamuzic[13], G. Mancini[54], M.N. Mancini[27], G. Manco[74a,74b], J.P. Mandalia[96], S.S. Mandarry[150], I. Mandić[95], L. Manhaes de Andrade Filho[84a], I.M. Maniatis[172], J. Manjarres Ramos[91], D.C. Mankad[172], A. Mann[111], S. Manzoni[37], L. Mao[63c], X. Mapekula[34c], A. Marantis[156,s], G. Marchiori[5], M. Marcisovsky[134], C. Marcon[72a], M. Marinescu[21], S. Marium[49], M. Marjanovic[123], A. Markhoos[55], M. Markovitch[67], E.J. Marshall[93], Z. Marshall[18a], S. Marti-Garcia[166], J. Martin[98], T.A. Martin[137], V.J. Martin[53], B. Martin dit Latour[17], L. Martinelli[76a,76b], M. Martinez[13,u], P. Martinez Agullo[166], V.I. Martinez Outschoorn[105], P. Martinez Suarez[13], S. Martin-Haugh[137], G. Martinovicova[136], V.S. Martoiu[28b], A.C. Martyniuk[98], A. Marzin[37], D. Mascione[79a,79b], L. Masetti[102], J. Masik[103], A.L. Maslennikov[38], S.L. Mason[42], P. Massarotti[73a,73b], P. Mastrandrea[75a,75b], A. Mastroberardino[44b,44a], T. Masubuchi[127], T.T. Mathew[126], T. Mathisen[164], J. Matousek[136], D.M. Mattern[50], J. Maurer[28b], T. Maurin[60], A.J. Maury[67], B. Maček[95], D.A. Maximov[38], A.E. May[103], R. Mazini[152], I. Maznas[118], M. Mazza[109], S.M. Mazza[139], E. Mazzeo[72a,72b], C. Mc Ginn[30], J.P. Mc Gowan[168], S.P. Mc Kee[108], C.A. Mc Lean[6], C.C. McCracken[167], E.F. McDonald[107], A.E. McDougall[117], J.A. Mcfayden[150], R.P. McGovern[131], R.P. Mckenzie[34g], T.C. Mclachlan[49], D.J. Mclaughlin[98], S.J. McMahon[137], C.M. Mcpartland[94], R.A. McPherson[168,y], S. Mehlhase[111], A. Mehta[94], D. Melini[166], B.R. Mellado Garcia[34g], A.H. Melo[56], F. Meloni[49], A.M. Mendes Jacques Da Costa[103], H.Y. Meng[158], L. Meng[93], S. Menke[112], M. Mentink[37], E. Meoni[44b,44a], G. Mercado[118], S. Merianos[156], C. Merlassino[70a,70c], L. Merola[73a,73b], C. Meroni[72a,72b], J. Metcalfe[6], A.S. Mete[6], E. Meuser[102], C. Meyer[69], J-P. Meyer[138], R.P. Middleton[137], L. Mijović[53], G. Mikenberg[172], M. Mikestikova[134], M. Mikuž[95], H. Mildner[102], A. Milic[37], D.W. Miller[40], E.H. Miller[147], L.S. Miller[35], A. Milov[172], D.A. Milstead[48a,48b], T. Min[114a], A.A. Minaenko[38], I.A. Minashvili[153b], L. Mince[60], A.I. Mincer[120], B. Mindur[87a], M. Mineev[39], Y. Mino[89], L.M. Mir[13], M. Miralles Lopez[60], M. Mironova[18a], M.C. Missio[116], A. Mitra[170], V.A. Mitsou[166], Y. Mitsumori[113], O. Miu[158], P.S. Miyagawa[96], T. Mkrtchyan[64a], M. Mlinarevic[98], T. Mlinarevic[98], M. Mlynarikova[37], S. Mobius[20], P. Mogg[111], M.H. Mohamed Farook[115], A.F. Mohammed[14,114c], S. Mohapatra[42], G. Mokgatitswane[34g], L. Moleri[172], B. Mondal[145], S. Mondal[135], K. Mönig[49], E. Monnier[104], L. Monsonis Romero[166], J. Montejo Berlingen[13], A. Montella[48a,48b], M. Montella[122], F. Montereali[78a,78b], F. Monticelli[92], S. Monzani[70a,70c], A. Morancho Tarda[43], N. Morange[67], A.L. Moreira De Carvalho[49], M. Moreno Llácer[166], C. Moreno Martinez[57], J.M. Moreno Perez[23b], P. Morettini[58b], S. Morgenstern[37], M. Morii[62], M. Morinaga[157], M. Moritsu[90], F. Morodei[76a,76b], P. Moschovakos[37], B. Moser[129], M. Mosidze[153b], T. Moskalets[45], P. Moskvitina[116], J. Moss[32,k], P. Moszkowicz[87a],

JHEP07(2025)086

A. Moussa[36d], E.J.W. Moyse[105], O. Mtintsilana[34g], S. Muanza[104], J. Mueller[132], D. Muenstermann[93], R. Müller[37], G.A. Mullier[164], A.J. Mullin[33], J.J. Mullin[131], A.E. Mulski[62], D.P. Mungo[158], D. Munoz Perez[166], F.J. Munoz Sanchez[103], M. Murin[103], W.J. Murray[170,137], M. Muškinja[95], C. Mwewa[30], A.G. Myagkov[38,a], A.J. Myers[8], G. Myers[108], M. Myska[135], B.P. Nachman[18a], O. Nackenhorst[50], K. Nagai[129], K. Nagano[85], R. Nagasaka[157], J.L. Nagle[30,ah], E. Nagy[104], A.M. Nairz[37], Y. Nakahama[85], K. Nakamura[85], K. Nakkalil[5], H. Nanjo[127], E.A. Narayanan[45], I. Naryshkin[38], L. Nasella[72a,72b], M. Naseri[35], S. Nasri[119b], C. Nass[25], G. Navarro[23a], J. Navarro-Gonzalez[166], R. Nayak[155], A. Nayaz[19], P.Y. Nechaeva[38], S. Nechaeva[24b,24a], F. Nechansky[134], L. Nedic[129], T.J. Neep[21], A. Negri[74a,74b], M. Negrini[24b], C. Nellist[117], C. Nelson[106], K. Nelson[108], S. Nemecek[134], M. Nessi[37,h], M.S. Neubauer[165], F. Neuhaus[102], J. Neundorf[49], J. Newell[94], P.R. Newman[21], C.W. Ng[132], Y.W.Y. Ng[49], B. Ngair[119a], H.D.N. Nguyen[110], R.B. Nickerson[129], R. Nicolaidou[138], J. Nielsen[139], M. Niemeyer[56], J. Niermann[56], N. Nikiforou[37], V. Nikolaenko[38,a], I. Nikolic-Audit[130], K. Nikolopoulos[21], P. Nilsson[30], I. Ninca[49], G. Ninio[155], A. Nisati[76a], N. Nishu[2], R. Nisius[112], J-E. Nitschke[51], E.K. Nkadimeng[34g], T. Nobe[157], T. Nommensen[151], M.B. Norfolk[143], B.J. Norman[35], M. Noury[36a], J. Novak[95], T. Novak[95], L. Novotny[135], R. Novotny[115], L. Nozka[125], K. Ntekas[162], N.M.J. Nunes De Moura Junior[84b], J. Ocariz[130], A. Ochi[86], I. Ochoa[133a], S. Oerdek[49,v], J.T. Offermann[40], A. Ogrodnik[136], A. Oh[103], C.C. Ohm[148], H. Oide[85], R. Oishi[157], M.L. Ojeda[37], Y. Okumura[157], L.F. Oleiro Seabra[133a], I. Oleksiyuk[57], S.A. Olivares Pino[140d], G. Oliveira Correa[13], D. Oliveira Damazio[30], J.L. Oliver[162], Ö.O. Öncel[55], A.P. O'Neill[20], A. Onofre[133a,133e], P.U.E. Onyisi[11], M.J. Oreglia[40], G.E. Orellana[92], D. Orestano[78a,78b], N. Orlando[13], R.S. Orr[158], L.M. Osojnak[131], R. Ospanov[63a], Y. Osumi[113], G. Otero y Garzon[31], H. Otono[90], P.S. Ott[64a], G.J. Ottino[18a], M. Ouchrif[36d], F. Ould-Saada[128], T. Ovsiannikova[142], M. Owen[60], R.E. Owen[137], V.E. Ozcan[22a], F. Ozturk[88], N. Ozturk[8], S. Ozturk[83], H.A. Pacey[129], A. Pacheco Pages[13], C. Padilla Aranda[13], G. Padovano[76a,76b], S. Pagan Griso[18a], G. Palacino[69], A. Palazzo[71a,71b], J. Pampel[25], J. Pan[175], T. Pan[65a], D.K. Panchal[11], C.E. Pandini[117], J.G. Panduro Vazquez[137], H.D. Pandya[1], H. Pang[15], P. Pani[49], G. Panizzo[70a,70c], L. Panwar[130], L. Paolozzi[57], S. Parajuli[165], A. Paramonov[6], C. Paraskevopoulos[54], D. Paredes Hernandez[65b], A. Pareti[74a,74b], K.R. Park[42], T.H. Park[158], M.A. Parker[33], F. Parodi[58b,58a], E.W. Parrish[118], V.A. Parrish[53], J.A. Parsons[42], U. Parzefall[55], B. Pascual Dias[110], L. Pascual Dominguez[101], E. Pasqualucci[76a], S. Passaggio[58b], F. Pastore[97], P. Patel[88], U.M. Patel[52], J.R. Pater[103], T. Pauly[37], F. Pauwels[136], C.I. Pazos[161], M. Pedersen[128], R. Pedro[133a], S.V. Peleganchuk[38], O. Penc[37], E.A. Pender[53], S. Peng[15], G.D. Penn[175], K.E. Penski[111], M. Penzin[38], B.S. Peralva[84d], A.P. Pereira Peixoto[142], L. Pereira Sanchez[147], D.V. Perepelitsa[30,ah], G. Perera[105], E. Perez Codina[159a], M. Perganti[10], H. Pernegger[37], S. Perrella[76a,76b], O. Perrin[41], K. Peters[49], R.F.Y. Peters[103], B.A. Petersen[37], T.C. Petersen[43], E. Petit[104], V. Petousis[135], C. Petridou[156,e], T. Petru[136], A. Petrukhin[145], M. Pettee[18a], A. Petukhov[38], K. Petukhova[37], R. Pezoa[140f], L. Pezzotti[37], G. Pezzullo[175], A.J. Pfleger[37], T.M. Pham[173], T. Pham[107], P.W. Phillips[137], G. Piacquadio[149], E. Pianori[18a], F. Piazza[126], R. Piegaia[31],

D. Pietreanu[28b], A.D. Pilkington[103], M. Pinamonti[70a,70c], J.L. Pinfold[2], B.C. Pinheiro Pereira[133a], J. Pinol Bel[13], A.E. Pinto Pinoargote[138,138], L. Pintucci[70a,70c], K.M. Piper[150], A. Pirttikoski[57], D.A. Pizzi[35], L. Pizzimento[65b], A. Pizzini[117], M.-A. Pleier[30], V. Pleskot[136], E. Plotnikova[39], G. Poddar[96], R. Poettgen[100], L. Poggioli[130], I. Pokharel[56], S. Polacek[136], G. Polesello[74a], A. Poley[146,159a], A. Polini[24b], C.S. Pollard[170], Z.B. Pollock[122], E. Pompa Pacchi[76a,76b], N.I. Pond[98], D. Ponomarenko[69], L. Pontecorvo[37], S. Popa[28a], G.A. Popeneciu[28d], A. Poreba[37], D.M. Portillo Quintero[159a], S. Pospisil[135], M.A. Postill[143], P. Postolache[28c], K. Potamianos[170], P.A. Potepa[87a], I.N. Potrap[39], C.J. Potter[33], H. Potti[151], J. Poveda[166], M.E. Pozo Astigarraga[37], A. Prades Ibanez[77a,77b], J. Pretel[168], D. Price[103], M. Primavera[71a], L. Primomo[70a,70c], M.A. Principe Martin[101], R. Privara[125], T. Procter[60], M.L. Proffitt[142], N. Proklova[131], K. Prokofiev[65c], G. Proto[112], J. Proudfoot[6], M. Przybycien[87a], W.W. Przygoda[87b], A. Psallidas[47], J.E. Puddefoot[143], D. Pudzha[55], D. Pyatiizbyantseva[38], J. Qian[108], D. Qichen[103], Y. Qin[13], T. Qiu[53], A. Quadt[56], M. Queitsch-Maitland[103], G. Quetant[57], R.P. Quinn[167], G. Rabanal Bolanos[62], D. Rafanoharana[55], F. Raffaeli[77a,77b], F. Ragusa[72a,72b], J.L. Rainbolt[40], J.A. Raine[57], S. Rajagopalan[30], E. Ramakoti[38], L. Rambelli[58b,58a], I.A. Ramirez-Berend[35], K. Ran[49,114c], D.S. Rankin[131], N.P. Rapheeha[34g], H. Rasheed[28b], V. Raskina[130], D.F. Rassloff[64a], A. Rastogi[18a], S. Rave[102], S. Ravera[58b,58a], B. Ravina[56], I. Ravinovich[172], M. Raymond[37], A.L. Read[128], N.P. Readioff[143], D.M. Rebuzzi[74a,74b], G. Redlinger[30], A.S. Reed[112], K. Reeves[27], J.A. Reidelsturz[174], D. Reikher[126], A. Rej[50], C. Rembser[37], M. Renda[28b], F. Renner[49], A.G. Rennie[162], A.L. Rescia[49], S. Resconi[72a], M. Ressegotti[58b,58a], S. Rettie[37], J.G. Reyes Rivera[109], E. Reynolds[18a], O.L. Rezanova[38], P. Reznicek[136], H. Riani[36d], N. Ribaric[52], E. Ricci[79a,79b], R. Richter[112], S. Richter[48a,48b], E. Richter-Was[87b], M. Ridel[130], S. Ridouani[36d], P. Rieck[120], P. Riedler[37], E.M. Riefel[48a,48b], J.O. Rieger[117], M. Rijssenbeek[149], M. Rimoldi[37], L. Rinaldi[24b,24a], P. Rincke[56], T.T. Rinn[30], M.P. Rinnagel[111], G. Ripellino[164], I. Riu[13], J.C. Rivera Vergara[168], F. Rizatdinova[124], E. Rizvi[96], B.R. Roberts[18a], S.S. Roberts[139], S.H. Robertson[106,y], D. Robinson[33], M. Robles Manzano[102], A. Robson[60], A. Rocchi[77a,77b], C. Roda[75a,75b], S. Rodriguez Bosca[37], Y. Rodriguez Garcia[23a], A. Rodriguez Rodriguez[55], A.M. Rodríguez Vera[118], S. Roe[37], J.T. Roemer[37], A.R. Roepe-Gier[139], O. Røhne[128], R.A. Rojas[105], C.P.A. Roland[130], J. Roloff[30], A. Romaniouk[80], E. Romano[74a,74b], M. Romano[24b], A.C. Romero Hernandez[165], N. Rompotis[94], L. Roos[130], S. Rosati[76a], B.J. Rosser[40], E. Rossi[129], E. Rossi[73a,73b], L.P. Rossi[62], L. Rossini[55], R. Rosten[122], M. Rotaru[28b], B. Rottler[55], C. Rougier[91], D. Rousseau[67], D. Rousso[49], A. Roy[165], S. Roy-Garand[158], A. Rozanov[104], Z.M.A. Rozario[60], Y. Rozen[154], A. Rubio Jimenez[166], A.J. Ruby[94], V.H. Ruelas Rivera[19], T.A. Ruggeri[1], A. Ruggiero[129], A. Ruiz-Martinez[166], A. Rummler[37], Z. Rurikova[55], N.A. Rusakovich[39], H.L. Russell[168], G. Russo[76a,76b], J.P. Rutherfoord[7], S. Rutherford Colmenares[33], M. Rybar[136], E.B. Rye[128], A. Ryzhov[45], J.A. Sabater Iglesias[57], H.F-W. Sadrozinski[139], F. Safai Tehrani[76a], B. Safarzadeh Samani[137], S. Saha[1], M. Sahinsoy[83], A. Saibel[166], M. Saimpert[138], M. Saito[157], T. Saito[157], A. Sala[72a,72b], D. Salamani[37], A. Salnikov[147], J. Salt[166], A. Salvador Salas[155], D. Salvatore[44b,44a], F. Salvatore[150], A. Salzburger[37], D. Sammel[55], E. Sampson[93],

D. Sampsonidis[156,e], D. Sampsonidou[126], J. Sánchez[166], V. Sanchez Sebastian[166], H. Sandaker[128], C.O. Sander[49], J.A. Sandesara[105], M. Sandhoff[174], C. Sandoval[23b], L. Sanfilippo[64a], D.P.C. Sankey[137], T. Sano[89], A. Sansoni[54], L. Santi[37,76b], C. Santoni[41], H. Santos[133a,133b], A. Santra[172], E. Sanzani[24b,24a], K.A. Saoucha[163], J.G. Saraiva[133a,133d], J. Sardain[7], O. Sasaki[85], K. Sato[160], C. Sauer[64b], E. Sauvan[4], P. Savard[158,af], R. Sawada[157], C. Sawyer[137], L. Sawyer[99], C. Sbarra[24b], A. Sbrizzi[24b,24a], T. Scanlon[98], J. Schaarschmidt[142], U. Schäfer[102], A.C. Schaffer[67,45], D. Schaile[111], R.D. Schamberger[149], C. Scharf[19], M.M. Schefer[20], V.A. Schegelsky[38], D. Scheirich[136], M. Schernau[162], C. Scheulen[56], C. Schiavi[58b,58a], M. Schioppa[44b,44a], B. Schlag[147], S. Schlenker[37], J. Schmeing[174], M.A. Schmidt[174], K. Schmieden[102], C. Schmitt[102], N. Schmitt[102], S. Schmitt[49], L. Schoeffel[138], A. Schoening[64b], P.G. Scholer[35], E. Schopf[129], M. Schott[25], J. Schovancova[37], S. Schramm[57], T. Schroer[57], H-C. Schultz-Coulon[64a], M. Schumacher[55], B.A. Schumm[139], Ph. Schune[138], A.J. Schuy[142], H.R. Schwartz[139], A. Schwartzman[147], T.A. Schwarz[108], Ph. Schwemling[138], R. Schwienhorst[109], F.G. Sciacca[20], A. Sciandra[30], G. Sciolla[27], F. Scuri[75a], C.D. Sebastiani[94], K. Sedlaczek[118], S.C. Seidel[115], A. Seiden[139], B.D. Seidlitz[42], C. Seitz[49], J.M. Seixas[84b], G. Sekhniaidze[73a], L. Selem[61], N. Semprini-Cesari[24b,24a], D. Sengupta[57], V. Senthilkumar[166], L. Serin[67], M. Sessa[77a,77b], H. Severini[123], F. Sforza[58b,58a], A. Sfyrla[57], Q. Sha[14], E. Shabalina[56], A.H. Shah[33], R. Shaheen[148], J.D. Shahinian[131], D. Shaked Renous[172], L.Y. Shan[14], M. Shapiro[18a], A. Sharma[37], A.S. Sharma[167], P. Sharma[81], P.B. Shatalov[38], K. Shaw[150], S.M. Shaw[103], Q. Shen[63c], D.J. Sheppard[146], P. Sherwood[98], L. Shi[98], X. Shi[14], S. Shimizu[85], C.O. Shimmin[175], J.D. Shinner[97], I.P.J. Shipsey[129,*], S. Shirabe[90], M. Shiyakova[39,w], M.J. Shochet[40], D.R. Shope[128], B. Shrestha[123], S. Shrestha[122,ai], I. Shreyber[38], M.J. Shroff[168], P. Sicho[134], A.M. Sickles[165], E. Sideras Haddad[34g], A.C. Sidley[117], A. Sidoti[24b], F. Siegert[51], Dj. Sijacki[16], F. Sili[92], J.M. Silva[53], I. Silva Ferreira[84b], M.V. Silva Oliveira[30], S.B. Silverstein[48a], S. Simion[67], R. Simoniello[37], E.L. Simpson[103], H. Simpson[150], L.R. Simpson[108], S. Simsek[83], S. Sindhu[56], P. Sinervo[158], S. Singh[158], S. Sinha[49], S. Sinha[103], M. Sioli[24b,24a], I. Siral[37], E. Sitnikova[49], J. Sjölin[48a,48b], A. Skaf[56], E. Skorda[21], P. Skubic[123], M. Slawinska[88], V. Smakhtin[172], B.H. Smart[137], S.Yu. Smirnov[38], Y. Smirnov[38], L.N. Smirnova[38,a], O. Smirnova[100], A.C. Smith[42], D.R. Smith[162], E.A. Smith[40], J.L. Smith[103], R. Smith[147], M. Smizanska[93], K. Smolek[135], A.A. Snesarev[38], H.L. Snoek[117], S. Snyder[30], R. Sobie[168,y], A. Soffer[155], C.A. Solans Sanchez[37], E.Yu. Soldatov[38], U. Soldevila[166], A.A. Solodkov[38], S. Solomon[27], A. Soloshenko[39], K. Solovieva[55], O.V. Solovyanov[41], P. Sommer[51], A. Sonay[13], W.Y. Song[159b], A. Sopczak[135], A.L. Sopio[53], F. Sopkova[29b], J.D. Sorenson[115], I.R. Sotarriva Alvarez[141], V. Sothilingam[64a], O.J. Soto Sandoval[140c,140b], S. Sottocornola[69], R. Soualah[163], Z. Soumaimi[36e], D. South[49], N. Soybelman[172], S. Spagnolo[71a,71b], M. Spalla[112], D. Sperlich[55], G. Spigo[37], B. Spisso[73a,73b], D.P. Spiteri[60], M. Spousta[136], E.J. Staats[35], R. Stamen[64a], A. Stampekis[21], E. Stanecka[88], W. Stanek-Maslouska[49], M.V. Stange[51], B. Stanislaus[18a], M.M. Stanitzki[49], B. Stapf[49], E.A. Starchenko[38], G.H. Stark[139], J. Stark[91], P. Staroba[134], P. Starovoitov[64a], S. Stärz[106], R. Staszewski[88], G. Stavropoulos[47], A. Stefl[37], P. Steinberg[30], B. Stelzer[146,159a], H.J. Stelzer[132], O. Stelzer-Chilton[159a], H. Stenzel[59], T.J. Stevenson[150], G.A. Stewart[37], J.R. Stewart[124],

M.C. Stockton[37], G. Stoicea[28b], M. Stolarski[133a], S. Stonjek[112], A. Straessner[51],
J. Strandberg[148], S. Strandberg[48a,48b], M. Stratmann[174], M. Strauss[123], T. Strebler[104],
P. Strizenec[29b], R. Ströhmer[169], D.M. Strom[126], R. Stroynowski[45], A. Strubig[48a,48b],
S.A. Stucci[30], B. Stugu[17], J. Stupak[123], N.A. Styles[49], D. Su[147], S. Su[63a], W. Su[63d],
X. Su[63a], D. Suchy[29a], K. Sugizaki[157], V.V. Sulin[38], M.J. Sullivan[94], D.M.S. Sultan[129],
L. Sultanaliyeva[38], S. Sultansoy[3b], T. Sumida[89], S. Sun[173], O. Sunneborn Gudnadottir[164],
N. Sur[104], M.R. Sutton[150], H. Suzuki[160], M. Svatos[134], M. Swiatlowski[159a],
T. Swirski[169], I. Sykora[29a], M. Sykora[136], T. Sykora[136], D. Ta[102], K. Tackmann[49,v],
A. Taffard[162], R. Tafirout[159a], J.S. Tafoya Vargas[67], Y. Takubo[85], M. Talby[104],
A.A. Talyshev[38], K.C. Tam[65b], N.M. Tamir[155], A. Tanaka[157], J. Tanaka[157],
R. Tanaka[67], M. Tanasini[149], Z. Tao[167], S. Tapia Araya[140f], S. Tapprogge[102],
A. Tarek Abouelfadl Mohamed[109], S. Tarem[154], K. Tariq[14], G. Tarna[28b], G.F. Tartarelli[72a],
M.J. Tartarin[91], P. Tas[136], M. Tasevsky[134], E. Tassi[44b,44a], A.C. Tate[165], G. Tateno[157],
Y. Tayalati[36e,x], G.N. Taylor[107], W. Taylor[159b], R. Teixeira De Lima[147],
P. Teixeira-Dias[97], J.J. Teoh[158], K. Terashi[157], J. Terron[101], S. Terzo[13], M. Testa[54],
R.J. Teuscher[158,y], A. Thaler[80], O. Theiner[57], T. Theveneaux-Pelzer[104], O. Thielmann[174],
D.W. Thomas[97], J.P. Thomas[21], E.A. Thompson[18a], P.D. Thompson[21], E. Thomson[131],
R.E. Thornberry[45], C. Tian[63a], Y. Tian[57], V. Tikhomirov[38,a], Yu.A. Tikhonov[38],
S. Timoshenko[38], D. Timoshyn[136], E.X.L. Ting[1], P. Tipton[175], A. Tishelman-Charny[30],
S.H. Tlou[34g], K. Todome[141], S. Todorova-Nova[136], S. Todt[51], L. Toffolin[70a,70c],
M. Togawa[85], J. Tojo[90], S. Tokár[29a], K. Tokushuku[85], O. Toldaiev[69], M. Tomoto[85,113],
L. Tompkins[147,m], K.W. Topolnicki[87b], E. Torrence[126], H. Torres[91], E. Torró Pastor[166],
M. Toscani[31], C. Tosciri[40], M. Tost[11], D.R. Tovey[143], I.S. Trandafir[28b], T. Trefzger[169],
A. Tricoli[30], I.M. Trigger[159a], S. Trincaz-Duvoid[130], D.A. Trischuk[27], B. Trocmé[61],
A. Tropina[39], L. Truong[34c], M. Trzebinski[88], A. Trzupek[88], F. Tsai[149], M. Tsai[108],
A. Tsiamis[156], P.V. Tsiareshka[38], S. Tsigaridas[159a], A. Tsirigotis[156,s], V. Tsiskaridze[158],
E.G. Tskhadadze[153a], M. Tsopoulou[156], Y. Tsujikawa[89], I.I. Tsukerman[38], V. Tsulaia[18a],
S. Tsuno[85], K. Tsuri[121], D. Tsybychev[149], Y. Tu[65b], A. Tudorache[28b], V. Tudorache[28b],
A.N. Tuna[62], S. Turchikhin[58b,58a], I. Turk Cakir[3a], R. Turra[72a], T. Turtuvshin[39,z],
P.M. Tuts[42], S. Tzamarias[156,e], E. Tzovara[102], F. Ukegawa[160], P.A. Ulloa Poblete[140c,140b],
E.N. Umaka[30], G. Unal[37], A. Undrus[30], G. Unel[162], J. Urban[29b], P. Urrejola[140a],
G. Usai[8], R. Ushioda[141], M. Usman[110], F. Ustuner[53], Z. Uysal[83], V. Vacek[135],
B. Vachon[106], T. Vafeiadis[37], A. Vaitkus[98], C. Valderanis[111], E. Valdes Santurio[48a,48b],
M. Valente[159a], S. Valentinetti[24b,24a], A. Valero[166], E. Valiente Moreno[166], A. Vallier[91],
J.A. Valls Ferrer[166], D.R. Van Arneman[117], T.R. Van Daalen[142], A. Van Der Graaf[50],
P. Van Gemmeren[6], M. Van Rijnbach[37], S. Van Stroud[98], I. Van Vulpen[117], P. Vana[136],
M. Vanadia[77a,77b], U.M. Vande Voorde[148], W. Vandelli[37], E.R. Vandewall[124],
D. Vannicola[155], L. Vannoli[54], R. Vari[76a], E.W. Varnes[7], C. Varni[18b], T. Varol[152],
D. Varouchas[67], L. Variale[166], K.E. Varvell[151], M.E. Vasile[28b], L. Vaslin[85],
G.A. Vasquez[168], A. Vasyukov[39], L.M. Vaughan[124], R. Vavricka[102], T. Vazquez Schroeder[37],
J. Veatch[32], V. Vecchio[103], M.J. Veen[105], I. Veliscek[30], L.M. Veloce[158], F. Veloso[133a,133c],
S. Veneziano[76a], A. Ventura[71a,71b], S. Ventura Gonzalez[138], A. Verbytskyi[112],
M. Verducci[75a,75b], C. Vergis[96], M. Verissimo De Araujo[84b], W. Verkerke[117],

J.C. Vermeulen[117], C. Vernieri[147], M. Vessella[105], M.C. Vetterli[146,af], A. Vgenopoulos[102], N. Viaux Maira[140f], T. Vickey[143], O.E. Vickey Boeriu[143], G.H.A. Viehhauser[129], L. Vigani[64b], M. Vigl[112], M. Villa[24b,24a], M. Villaplana Perez[166], E.M. Villhauer[53], E. Vilucchi[54], M.G. Vincter[35], A. Visibile[117], C. Vittori[37], I. Vivarelli[24b,24a], E. Voevodina[112], F. Vogel[111], J.C. Voigt[51], P. Vokac[135], Yu. Volkotrub[87b], E. Von Toerne[25], B. Vormwald[37], V. Vorobel[136], K. Vorobev[38], M. Vos[166], K. Voss[145], M. Vozak[117], L. Vozdecky[123], N. Vranjes[16], M. Vranjes Milosavljevic[16], M. Vreeswijk[117], N.K. Vu[63d,63c], R. Vuillermet[37], O. Vujinovic[102], I. Vukotic[40], I.K. Vyas[35], S. Wada[160], C. Wagner[147], J.M. Wagner[18a], W. Wagner[174], S. Wahdan[174], H. Wahlberg[92], J. Walder[137], R. Walker[111], W. Walkowiak[145], A. Wall[131], E.J. Wallin[100], T. Wamorkar[6], A.Z. Wang[139], C. Wang[102], C. Wang[11], H. Wang[18a], J. Wang[65c], P. Wang[98], R. Wang[62], R. Wang[6], S.M. Wang[152], S. Wang[63b], S. Wang[14], T. Wang[63a], W.T. Wang[81], W. Wang[14], X. Wang[114a], X. Wang[165], X. Wang[63c], Y. Wang[63d], Y. Wang[114a], Y. Wang[63a], Z. Wang[108], Z. Wang[63d,52,63c], Z. Wang[108], A. Warburton[106], R.J. Ward[21], N. Warrack[60], S. Waterhouse[97], A.T. Watson[21], H. Watson[53], M.F. Watson[21], E. Watton[60,137], G. Watts[142], B.M. Waugh[98], J.M. Webb[55], C. Weber[30], H.A. Weber[19], M.S. Weber[20], S.M. Weber[64a], C. Wei[63a], Y. Wei[55], A.R. Weidberg[129], E.J. Weik[120], J. Weingarten[50], C. Weiser[55], C.J. Wells[49], T. Wenaus[30], B. Wendland[50], T. Wengler[37], N.S. Wenke[112], N. Wermes[25], M. Wessels[64a], A.M. Wharton[93], A.S. White[62], A. White[8], M.J. White[1], D. Whiteson[162], L. Wickremasinghe[127], W. Wiedenmann[173], M. Wielers[137], C. Wiglesworth[43], D.J. Wilbern[123], H.G. Wilkens[37], J.J.H. Wilkinson[33], D.M. Williams[42], H.H. Williams[131], S. Williams[33], S. Willocq[105], B.J. Wilson[103], P.J. Windischhofer[40], F.I. Winkel[31], F. Winklmeier[126], B.T. Winter[55], J.K. Winter[103], M. Wittgen[147], M. Wobisch[99], T. Wojtkowski[61], Z. Wolffs[117], J. Wollrath[162], M.W. Wolter[88], H. Wolters[133a,133c], M.C. Wong[139], E.L. Woodward[42], S.D. Worm[49], B.K. Wosiek[88], K.W. Woźniak[88], S. Wozniewski[56], K. Wraight[60], C. Wu[21], M. Wu[114b], M. Wu[116], S.L. Wu[173], X. Wu[57], Y. Wu[63a], Z. Wu[4], J. Wuerzinger[112,ad], T.R. Wyatt[103], B.M. Wynne[53], S. Xella[43], L. Xia[114a], M. Xia[15], M. Xie[63a], S. Xin[14,114c], A. Xiong[126], J. Xiong[18a], D. Xu[14], H. Xu[63a], L. Xu[63a], R. Xu[131], T. Xu[108], Y. Xu[15], Z. Xu[53], Z. Xu[114a], B. Yabsley[151], S. Yacoob[34a], Y. Yamaguchi[85], E. Yamashita[157], H. Yamauchi[160], T. Yamazaki[18a], Y. Yamazaki[86], S. Yan[60], Z. Yan[105], H.J. Yang[63c,63d], H.T. Yang[63a], S. Yang[63a], T. Yang[65c], X. Yang[37], X. Yang[14], Y. Yang[45], Y. Yang[63a], Z. Yang[63a], W-M. Yao[18a], H. Ye[114a], H. Ye[56], J. Ye[14], S. Ye[30], X. Ye[63a], Y. Yeh[98], I. Yeletskikh[39], B. Yeo[18b], M.R. Yexley[98], T.P. Yildirim[129], P. Yin[42], K. Yorita[171], S. Younas[28b], C.J.S. Young[37], C. Young[147], C. Yu[14,114c], Y. Yu[63a], J. Yuan[14,114c], M. Yuan[108], R. Yuan[63d,63c], L. Yue[98], M. Zaazoua[63a], B. Zabinski[88], E. Zaid[53], Z.K. Zak[88], T. Zakareishvili[166], S. Zambito[57], J.A. Zamora Saa[140d,140b], J. Zang[157], D. Zanzi[55], O. Zaplatilek[135], C. Zeitnitz[174], H. Zeng[14], J.C. Zeng[165], D.T. Zenger Jr[27], O. Zenin[38], T. Ženiš[29a], S. Zenz[96], S. Zerradi[36a], D. Zerwas[67], M. Zhai[14,114c], D.F. Zhang[143], J. Zhang[63b], J. Zhang[6], K. Zhang[14,114c], L. Zhang[63a], L. Zhang[114a], P. Zhang[14,114c], R. Zhang[173], S. Zhang[108], S. Zhang[91], T. Zhang[157], X. Zhang[63c], X. Zhang[63b], Y. Zhang[63c], Y. Zhang[98], Y. Zhang[114a], Z. Zhang[18a], Z. Zhang[63b], Z. Zhang[67], H. Zhao[142], T. Zhao[63b],

JHEP07(2025)086

Y. Zhao[139], Z. Zhao[63a], Z. Zhao[63a], A. Zhemchugov[39], J. Zheng[114a], K. Zheng[165], X. Zheng[63a], Z. Zheng[147], D. Zhong[165], B. Zhou[108], H. Zhou[7], N. Zhou[63c], Y. Zhou[15], Y. Zhou[114a], Y. Zhou[7], C.G. Zhu[63b], J. Zhu[108], X. Zhu[63d], Y. Zhu[63c], Y. Zhu[63a], X. Zhuang[14], K. Zhukov[69], N.I. Zimine[39], J. Zinsser[64b], M. Ziolkowski[145], L. Živković[16], A. Zoccoli[24b,24a], K. Zoch[62], T.G. Zorbas[143], O. Zormpa[47], W. Zou[42], L. Zwalinski[37]

[1] *Department of Physics, University of Adelaide, Adelaide; Australia*
[2] *Department of Physics, University of Alberta, Edmonton AB; Canada*
[3] [(a)] *Department of Physics, Ankara University, Ankara;*[(b)] *Division of Physics, TOBB University of Economics and Technology, Ankara; Türkiye*
[4] *LAPP, Université Savoie Mont Blanc, CNRS/IN2P3, Annecy; France*
[5] *APC, Université Paris Cité, CNRS/IN2P3, Paris; France*
[6] *High Energy Physics Division, Argonne National Laboratory, Argonne IL; United States of America*
[7] *Department of Physics, University of Arizona, Tucson AZ; United States of America*
[8] *Department of Physics, University of Texas at Arlington, Arlington TX; United States of America*
[9] *Physics Department, National and Kapodistrian University of Athens, Athens; Greece*
[10] *Physics Department, National Technical University of Athens, Zografou; Greece*
[11] *Department of Physics, University of Texas at Austin, Austin TX; United States of America*
[12] *Institute of Physics, Azerbaijan Academy of Sciences, Baku; Azerbaijan*
[13] *Institut de Física d'Altes Energies (IFAE), Barcelona Institute of Science and Technology, Barcelona; Spain*
[14] *Institute of High Energy Physics, Chinese Academy of Sciences, Beijing; China*
[15] *Physics Department, Tsinghua University, Beijing; China*
[16] *Institute of Physics, University of Belgrade, Belgrade; Serbia*
[17] *Department for Physics and Technology, University of Bergen, Bergen; Norway*
[18] [(a)] *Physics Division, Lawrence Berkeley National Laboratory, Berkeley CA;*[(b)] *University of California, Berkeley CA; United States of America*
[19] *Institut für Physik, Humboldt Universität zu Berlin, Berlin; Germany*
[20] *Albert Einstein Center for Fundamental Physics and Laboratory for High Energy Physics, University of Bern, Bern; Switzerland*
[21] *School of Physics and Astronomy, University of Birmingham, Birmingham; United Kingdom*
[22] [(a)] *Department of Physics, Bogazici University, Istanbul;*[(b)] *Department of Physics Engineering, Gaziantep University, Gaziantep;*[(c)] *Department of Physics, Istanbul University, Istanbul; Türkiye*
[23] [(a)] *Facultad de Ciencias y Centro de Investigaciónes, Universidad Antonio Nariño, Bogotá;*[(b)] *Departamento de Física, Universidad Nacional de Colombia, Bogotá; Colombia*
[24] [(a)] *Dipartimento di Fisica e Astronomia A. Righi, Università di Bologna, Bologna;*[(b)] *INFN Sezione di Bologna; Italy*
[25] *Physikalisches Institut, Universität Bonn, Bonn; Germany*
[26] *Department of Physics, Boston University, Boston MA; United States of America*
[27] *Department of Physics, Brandeis University, Waltham MA; United States of America*
[28] [(a)] *Transilvania University of Brasov, Brasov;*[(b)] *Horia Hulubei National Institute of Physics and Nuclear Engineering, Bucharest;*[(c)] *Department of Physics, Alexandru Ioan Cuza University of Iasi, Iasi;*[(d)] *National Institute for Research and Development of Isotopic and Molecular Technologies, Physics Department, Cluj-Napoca;*[(e)] *National University of Science and Technology Politechnica, Bucharest;*[(f)] *West University in Timisoara, Timisoara;*[(g)] *Faculty of Physics, University of Bucharest, Bucharest; Romania*
[29] [(a)] *Faculty of Mathematics, Physics and Informatics, Comenius University, Bratislava;*[(b)] *Department of Subnuclear Physics, Institute of Experimental Physics of the Slovak Academy of Sciences, Kosice; Slovak Republic*
[30] *Physics Department, Brookhaven National Laboratory, Upton NY; United States of America*
[31] *Universidad de Buenos Aires, Facultad de Ciencias Exactas y Naturales, Departamento de Física, y CONICET, Instituto de Física de Buenos Aires (IFIBA), Buenos Aires; Argentina*
[32] *California State University, CA; United States of America*
[33] *Cavendish Laboratory, University of Cambridge, Cambridge; United Kingdom*

JHEP07(2025)086

[34] [(a)] Department of Physics, University of Cape Town, Cape Town; [(b)] iThemba Labs, Western Cape; [(c)] Department of Mechanical Engineering Science, University of Johannesburg, Johannesburg; [(d)] National Institute of Physics, University of the Philippines Diliman (Philippines); [(e)] University of South Africa, Department of Physics, Pretoria; [(f)] University of Zululand, KwaDlangezwa; [(g)] School of Physics, University of the Witwatersrand, Johannesburg; South Africa
[35] Department of Physics, Carleton University, Ottawa ON; Canada
[36] [(a)] Faculté des Sciences Ain Chock, Université Hassan II de Casablanca; [(b)] Faculté des Sciences, Université Ibn-Tofail, Kénitra; [(c)] Faculté des Sciences Semlalia, Université Cadi Ayyad, LPHEA-Marrakech; [(d)] LPMR, Faculté des Sciences, Université Mohamed Premier, Oujda; [(e)] Faculté des sciences, Université Mohammed V, Rabat; [(f)] Institute of Applied Physics, Mohammed VI Polytechnic University, Ben Guerir; Morocco
[37] CERN, Geneva; Switzerland
[38] Affiliated with an institute covered by a cooperation agreement with CERN
[39] Affiliated with an international laboratory covered by a cooperation agreement with CERN
[40] Enrico Fermi Institute, University of Chicago, Chicago IL; United States of America
[41] LPC, Université Clermont Auvergne, CNRS/IN2P3, Clermont-Ferrand; France
[42] Nevis Laboratory, Columbia University, Irvington NY; United States of America
[43] Niels Bohr Institute, University of Copenhagen, Copenhagen; Denmark
[44] [(a)] Dipartimento di Fisica, Università della Calabria, Rende; [(b)] INFN Gruppo Collegato di Cosenza, Laboratori Nazionali di Frascati; Italy
[45] Physics Department, Southern Methodist University, Dallas TX; United States of America
[46] Physics Department, University of Texas at Dallas, Richardson TX; United States of America
[47] National Centre for Scientific Research "Demokritos", Agia Paraskevi; Greece
[48] [(a)] Department of Physics, Stockholm University; [(b)] Oskar Klein Centre, Stockholm; Sweden
[49] Deutsches Elektronen-Synchrotron DESY, Hamburg and Zeuthen; Germany
[50] Fakultät Physik , Technische Universität Dortmund, Dortmund; Germany
[51] Institut für Kern- und Teilchenphysik, Technische Universität Dresden, Dresden; Germany
[52] Department of Physics, Duke University, Durham NC; United States of America
[53] SUPA — School of Physics and Astronomy, University of Edinburgh, Edinburgh; United Kingdom
[54] INFN e Laboratori Nazionali di Frascati, Frascati; Italy
[55] Physikalisches Institut, Albert-Ludwigs-Universität Freiburg, Freiburg; Germany
[56] II. Physikalisches Institut, Georg-August-Universität Göttingen, Göttingen; Germany
[57] Département de Physique Nucléaire et Corpusculaire, Université de Genève, Genève; Switzerland
[58] [(a)] Dipartimento di Fisica, Università di Genova, Genova; [(b)] INFN Sezione di Genova; Italy
[59] II. Physikalisches Institut, Justus-Liebig-Universität Giessen, Giessen; Germany
[60] SUPA — School of Physics and Astronomy, University of Glasgow, Glasgow; United Kingdom
[61] LPSC, Université Grenoble Alpes, CNRS/IN2P3, Grenoble INP, Grenoble; France
[62] Laboratory for Particle Physics and Cosmology, Harvard University, Cambridge MA; United States of America
[63] [(a)] Department of Modern Physics and State Key Laboratory of Particle Detection and Electronics, University of Science and Technology of China, Hefei; [(b)] Institute of Frontier and Interdisciplinary Science and Key Laboratory of Particle Physics and Particle Irradiation (MOE), Shandong University, Qingdao; [(c)] State Key Laboratory of Dark Matter Physics, School of Physics and Astronomy, Shanghai Jiao Tong University, Key Laboratory for Particle Astrophysics and Cosmology (MOE), SKLPPC, Shanghai; [(d)] State Key Laboratory of Dark Matter Physics, Tsung-Dao Lee Institute, Shanghai Jiao Tong University, Shanghai; [(e)] School of Physics, Zhengzhou University; China
[64] [(a)] Kirchhoff-Institut für Physik, Ruprecht-Karls-Universität Heidelberg, Heidelberg; [(b)] Physikalisches Institut, Ruprecht-Karls-Universität Heidelberg, Heidelberg; Germany
[65] [(a)] Department of Physics, Chinese University of Hong Kong, Shatin, N.T., Hong Kong; [(b)] Department of Physics, University of Hong Kong, Hong Kong; [(c)] Department of Physics and Institute for Advanced Study, Hong Kong University of Science and Technology, Clear Water Bay, Kowloon, Hong Kong; China
[66] Department of Physics, National Tsing Hua University, Hsinchu; Taiwan
[67] IJCLab, Université Paris-Saclay, CNRS/IN2P3, 91405, Orsay; France
[68] Centro Nacional de Microelectrónica (IMB-CNM-CSIC), Barcelona; Spain
[69] Department of Physics, Indiana University, Bloomington IN; United States of America

[70] [(a)] *INFN Gruppo Collegato di Udine, Sezione di Trieste, Udine;*[(b)] *ICTP, Trieste;*[(c)] *Dipartimento Politecnico di Ingegneria e Architettura, Università di Udine, Udine; Italy*
[71] [(a)] *INFN Sezione di Lecce;*[(b)] *Dipartimento di Matematica e Fisica, Università del Salento, Lecce; Italy*
[72] [(a)] *INFN Sezione di Milano;*[(b)] *Dipartimento di Fisica, Università di Milano, Milano; Italy*
[73] [(a)] *INFN Sezione di Napoli;*[(b)] *Dipartimento di Fisica, Università di Napoli, Napoli; Italy*
[74] [(a)] *INFN Sezione di Pavia;*[(b)] *Dipartimento di Fisica, Università di Pavia, Pavia; Italy*
[75] [(a)] *INFN Sezione di Pisa;*[(b)] *Dipartimento di Fisica E. Fermi, Università di Pisa, Pisa; Italy*
[76] [(a)] *INFN Sezione di Roma;*[(b)] *Dipartimento di Fisica, Sapienza Università di Roma, Roma; Italy*
[77] [(a)] *INFN Sezione di Roma Tor Vergata;*[(b)] *Dipartimento di Fisica, Università di Roma Tor Vergata, Roma; Italy*
[78] [(a)] *INFN Sezione di Roma Tre;*[(b)] *Dipartimento di Matematica e Fisica, Università Roma Tre, Roma; Italy*
[79] [(a)] *INFN-TIFPA;*[(b)] *Università degli Studi di Trento, Trento; Italy*
[80] *Universität Innsbruck, Department of Astro and Particle Physics, Innsbruck; Austria*
[81] *University of Iowa, Iowa City IA; United States of America*
[82] *Department of Physics and Astronomy, Iowa State University, Ames IA; United States of America*
[83] *Istinye University, Sariyer, Istanbul; Türkiye*
[84] [(a)] *Departamento de Engenharia Elétrica, Universidade Federal de Juiz de Fora (UFJF), Juiz de Fora;*[(b)] *Universidade Federal do Rio De Janeiro COPPE/EE/IF, Rio de Janeiro;*[(c)] *Instituto de Física, Universidade de São Paulo, São Paulo;*[(d)] *Rio de Janeiro State University, Rio de Janeiro;*[(e)] *Federal University of Bahia, Bahia; Brazil*
[85] *KEK, High Energy Accelerator Research Organization, Tsukuba; Japan*
[86] *Graduate School of Science, Kobe University, Kobe; Japan*
[87] [(a)] *AGH University of Krakow, Faculty of Physics and Applied Computer Science, Krakow;*[(b)] *Marian Smoluchowski Institute of Physics, Jagiellonian University, Krakow; Poland*
[88] *Institute of Nuclear Physics Polish Academy of Sciences, Krakow; Poland*
[89] *Faculty of Science, Kyoto University, Kyoto; Japan*
[90] *Research Center for Advanced Particle Physics and Department of Physics, Kyushu University, Fukuoka; Japan*
[91] *L2IT, Université de Toulouse, CNRS/IN2P3, UPS, Toulouse; France*
[92] *Instituto de Física La Plata, Universidad Nacional de La Plata and CONICET, La Plata; Argentina*
[93] *Physics Department, Lancaster University, Lancaster; United Kingdom*
[94] *Oliver Lodge Laboratory, University of Liverpool, Liverpool; United Kingdom*
[95] *Department of Experimental Particle Physics, Jožef Stefan Institute and Department of Physics, University of Ljubljana, Ljubljana; Slovenia*
[96] *Department of Physics and Astronomy, Queen Mary University of London, London; United Kingdom*
[97] *Department of Physics, Royal Holloway University of London, Egham; United Kingdom*
[98] *Department of Physics and Astronomy, University College London, London; United Kingdom*
[99] *Louisiana Tech University, Ruston LA; United States of America*
[100] *Fysiska institutionen, Lunds universitet, Lund; Sweden*
[101] *Departamento de Física Teorica C-15 and CIAFF, Universidad Autónoma de Madrid, Madrid; Spain*
[102] *Institut für Physik, Universität Mainz, Mainz; Germany*
[103] *School of Physics and Astronomy, University of Manchester, Manchester; United Kingdom*
[104] *CPPM, Aix-Marseille Université, CNRS/IN2P3, Marseille; France*
[105] *Department of Physics, University of Massachusetts, Amherst MA; United States of America*
[106] *Department of Physics, McGill University, Montreal QC; Canada*
[107] *School of Physics, University of Melbourne, Victoria; Australia*
[108] *Department of Physics, University of Michigan, Ann Arbor MI; United States of America*
[109] *Department of Physics and Astronomy, Michigan State University, East Lansing MI; United States of America*
[110] *Group of Particle Physics, University of Montreal, Montreal QC; Canada*
[111] *Fakultät für Physik, Ludwig-Maximilians-Universität München, München; Germany*
[112] *Max-Planck-Institut für Physik (Werner-Heisenberg-Institut), München; Germany*
[113] *Graduate School of Science and Kobayashi-Maskawa Institute, Nagoya University, Nagoya; Japan*

JHEP07(2025)086

[114] (a) *Department of Physics, Nanjing University, Nanjing;* (b) *School of Science, Shenzhen Campus of Sun Yat-sen University;* (c) *University of Chinese Academy of Science (UCAS), Beijing; China*
[115] *Department of Physics and Astronomy, University of New Mexico, Albuquerque NM; United States of America*
[116] *Institute for Mathematics, Astrophysics and Particle Physics, Radboud University/Nikhef, Nijmegen; Netherlands*
[117] *Nikhef National Institute for Subatomic Physics and University of Amsterdam, Amsterdam; Netherlands*
[118] *Department of Physics, Northern Illinois University, DeKalb IL; United States of America*
[119] (a) *New York University Abu Dhabi, Abu Dhabi;* (b) *United Arab Emirates University, Al Ain; United Arab Emirates*
[120] *Department of Physics, New York University, New York NY; United States of America*
[121] *Ochanomizu University, Otsuka, Bunkyo-ku, Tokyo; Japan*
[122] *Ohio State University, Columbus OH; United States of America*
[123] *Homer L. Dodge Department of Physics and Astronomy, University of Oklahoma, Norman OK; United States of America*
[124] *Department of Physics, Oklahoma State University, Stillwater OK; United States of America*
[125] *Palacký University, Joint Laboratory of Optics, Olomouc; Czech Republic*
[126] *Institute for Fundamental Science, University of Oregon, Eugene, OR; United States of America*
[127] *Graduate School of Science, University of Osaka, Osaka; Japan*
[128] *Department of Physics, University of Oslo, Oslo; Norway*
[129] *Department of Physics, Oxford University, Oxford; United Kingdom*
[130] *LPNHE, Sorbonne Université, Université Paris Cité, CNRS/IN2P3, Paris; France*
[131] *Department of Physics, University of Pennsylvania, Philadelphia PA; United States of America*
[132] *Department of Physics and Astronomy, University of Pittsburgh, Pittsburgh PA; United States of America*
[133] (a) *Laboratório de Instrumentação e Física Experimental de Partículas — LIP, Lisboa;* (b) *Departamento de Física, Faculdade de Ciências, Universidade de Lisboa, Lisboa;* (c) *Departamento de Física, Universidade de Coimbra, Coimbra;* (d) *Centro de Física Nuclear da Universidade de Lisboa, Lisboa;* (e) *Departamento de Física, Escola de Ciências, Universidade do Minho, Braga;* (f) *Departamento de Física Teórica y del Cosmos, Universidad de Granada, Granada (Spain);* (g) *Departamento de Física, Instituto Superior Técnico, Universidade de Lisboa, Lisboa; Portugal*
[134] *Institute of Physics of the Czech Academy of Sciences, Prague; Czech Republic*
[135] *Czech Technical University in Prague, Prague; Czech Republic*
[136] *Charles University, Faculty of Mathematics and Physics, Prague; Czech Republic*
[137] *Particle Physics Department, Rutherford Appleton Laboratory, Didcot; United Kingdom*
[138] *IRFU, CEA, Université Paris-Saclay, Gif-sur-Yvette; France*
[139] *Santa Cruz Institute for Particle Physics, University of California Santa Cruz, Santa Cruz CA; United States of America*
[140] (a) *Departamento de Física, Pontificia Universidad Católica de Chile, Santiago;* (b) *Millennium Institute for Subatomic physics at high energy frontier (SAPHIR), Santiago;* (c) *Instituto de Investigación Multidisciplinario en Ciencia y Tecnología, y Departamento de Física, Universidad de La Serena;* (d) *Universidad Andres Bello, Department of Physics, Santiago;* (e) *Instituto de Alta Investigación, Universidad de Tarapacá, Arica;* (f) *Departamento de Física, Universidad Técnica Federico Santa María, Valparaíso; Chile*
[141] *Department of Physics, Institute of Science, Tokyo; Japan*
[142] *Department of Physics, University of Washington, Seattle WA; United States of America*
[143] *Department of Physics and Astronomy, University of Sheffield, Sheffield; United Kingdom*
[144] *Department of Physics, Shinshu University, Nagano; Japan*
[145] *Department Physik, Universität Siegen, Siegen; Germany*
[146] *Department of Physics, Simon Fraser University, Burnaby BC; Canada*
[147] *SLAC National Accelerator Laboratory, Stanford CA; United States of America*
[148] *Department of Physics, Royal Institute of Technology, Stockholm; Sweden*
[149] *Departments of Physics and Astronomy, Stony Brook University, Stony Brook NY; United States of America*

JHEP07(2025)086

[150] Department of Physics and Astronomy, University of Sussex, Brighton; United Kingdom
[151] School of Physics, University of Sydney, Sydney; Australia
[152] Institute of Physics, Academia Sinica, Taipei; Taiwan
[153] [(a)] E. Andronikashvili Institute of Physics, Iv. Javakhishvili Tbilisi State University, Tbilisi; [(b)] High Energy Physics Institute, Tbilisi State University, Tbilisi; [(c)] University of Georgia, Tbilisi; Georgia
[154] Department of Physics, Technion, Israel Institute of Technology, Haifa; Israel
[155] Raymond and Beverly Sackler School of Physics and Astronomy, Tel Aviv University, Tel Aviv; Israel
[156] Department of Physics, Aristotle University of Thessaloniki, Thessaloniki; Greece
[157] International Center for Elementary Particle Physics and Department of Physics, University of Tokyo, Tokyo; Japan
[158] Department of Physics, University of Toronto, Toronto ON; Canada
[159] [(a)] TRIUMF, Vancouver BC; [(b)] Department of Physics and Astronomy, York University, Toronto ON; Canada
[160] Division of Physics and Tomonaga Center for the History of the Universe, Faculty of Pure and Applied Sciences, University of Tsukuba, Tsukuba; Japan
[161] Department of Physics and Astronomy, Tufts University, Medford MA; United States of America
[162] Department of Physics and Astronomy, University of California Irvine, Irvine CA; United States of America
[163] University of Sharjah, Sharjah; United Arab Emirates
[164] Department of Physics and Astronomy, University of Uppsala, Uppsala; Sweden
[165] Department of Physics, University of Illinois, Urbana IL; United States of America
[166] Instituto de Física Corpuscular (IFIC), Centro Mixto Universidad de Valencia — CSIC, Valencia; Spain
[167] Department of Physics, University of British Columbia, Vancouver BC; Canada
[168] Department of Physics and Astronomy, University of Victoria, Victoria BC; Canada
[169] Fakultät für Physik und Astronomie, Julius-Maximilians-Universität Würzburg, Würzburg; Germany
[170] Department of Physics, University of Warwick, Coventry; United Kingdom
[171] Waseda University, Tokyo; Japan
[172] Department of Particle Physics and Astrophysics, Weizmann Institute of Science, Rehovot; Israel
[173] Department of Physics, University of Wisconsin, Madison WI; United States of America
[174] Fakultät für Mathematik und Naturwissenschaften, Fachgruppe Physik, Bergische Universität Wuppertal, Wuppertal; Germany
[175] Department of Physics, Yale University, New Haven CT; United States of America

[a] Also Affiliated with an institute covered by a cooperation agreement with CERN
[b] Also at An-Najah National University, Nablus; Palestine
[c] Also at Borough of Manhattan Community College, City University of New York, New York NY; United States of America
[d] Also at Center for High Energy Physics, Peking University; China
[e] Also at Center for Interdisciplinary Research and Innovation (CIRI-AUTH), Thessaloniki; Greece
[f] Also at CERN, Geneva; Switzerland
[g] Also at CMD-AC UNEC Research Center, Azerbaijan State University of Economics (UNEC); Azerbaijan
[h] Also at Département de Physique Nucléaire et Corpusculaire, Université de Genève, Genève; Switzerland
[i] Also at Departament de Fisica de la Universitat Autonoma de Barcelona, Barcelona; Spain
[j] Also at Department of Financial and Management Engineering, University of the Aegean, Chios; Greece
[k] Also at Department of Physics, California State University, Sacramento; United States of America
[l] Also at Department of Physics, King's College London, London; United Kingdom
[m] Also at Department of Physics, Stanford University, Stanford CA; United States of America
[n] Also at Department of Physics, Stellenbosch University; South Africa
[o] Also at Department of Physics, University of Fribourg, Fribourg; Switzerland
[p] Also at Department of Physics, University of Thessaly; Greece
[q] Also at Department of Physics, Westmont College, Santa Barbara; United States of America
[r] Also at Faculty of Physics, Sofia University, 'St. Kliment Ohridski', Sofia; Bulgaria
[s] Also at Hellenic Open University, Patras; Greece
[t] Also at Imam Mohammad Ibn Saud Islamic University; Saudi Arabia

JHEP07(2025)086

[u] *Also at Institucio Catalana de Recerca i Estudis Avancats, ICREA, Barcelona; Spain*
[v] *Also at Institut für Experimentalphysik, Universität Hamburg, Hamburg; Germany*
[w] *Also at Institute for Nuclear Research and Nuclear Energy (INRNE) of the Bulgarian Academy of Sciences, Sofia; Bulgaria*
[x] *Also at Institute of Applied Physics, Mohammed VI Polytechnic University, Ben Guerir; Morocco*
[y] *Also at Institute of Particle Physics (IPP); Canada*
[z] *Also at Institute of Physics and Technology, Mongolian Academy of Sciences, Ulaanbaatar; Mongolia*
[aa] *Also at Institute of Physics, Azerbaijan Academy of Sciences, Baku; Azerbaijan*
[ab] *Also at Institute of Theoretical Physics, Ilia State University, Tbilisi; Georgia*
[ac] *Also at National Institute of Physics, University of the Philippines Diliman (Philippines); Philippines*
[ad] *Also at Technical University of Munich, Munich; Germany*
[ae] *Also at The Collaborative Innovation Center of Quantum Matter (CICQM), Beijing; China*
[af] *Also at TRIUMF, Vancouver BC; Canada*
[ag] *Also at Università di Napoli Parthenope, Napoli; Italy*
[ah] *Also at University of Colorado Boulder, Department of Physics, Colorado; United States of America*
[ai] *Also at Washington College, Chestertown, MD; United States of America*
[aj] *Also at Yeditepe University, Physics Department, Istanbul; Türkiye*
[*] *Deceased*

JHEP07(2025)086